PERGAMON

International Journal of Solids and Structures 40 (2003) 1059–1088

INTERNATIONAL JOURNAL OF SOLIDS and STRUCTURES

www.elsevier.com/locate/ijsolstr

A nonlinear theory for doubly curved anisotropic sandwich shells with transversely compressible core

Jörg Hohe [a,*], Liviu Librescu [b]

[a] Universität Siegen, Institut für Mechanik und Regelungstechnik, Paul-Bonatz-Str. 9-11, D-57068 Siegen, Germany
[b] Virginia Polytechnic Institute and State University, Department of Engineering Science and Mechanics, Blacksburg, VA 24061-0219, USA

Received 13 June 2002; received in revised form 20 October 2002

Abstract

In the present paper, an advanced geometrically nonlinear shell theory of doubly curved structural sandwich panels with transversely compressible core is presented. The model is based on the adoption of the Kirchhoff theory for the face sheets and a second/third order power series expansion for the core displacements. The theory accounts for dynamic effects as well as for initial geometric imperfections. In the v. Kármán sense, large displacement theory is employed with respect to the transverse direction while the displacement gradients with respect to the tangential directions are assumed to be small. The equations of motion are derived by means of Hamilton's principle and hold valid for all types of elastic and elastic–plastic material models. The theory is illustrated by an analysis of the elastic buckling and postbuckling behavior of flat and curved sandwich panels using an extended Galerkin scheme. Owing to the assumed transverse flexibility of the core, both the global and the local (face wrinkling) instability modes can be addressed.

Keywords: Sandwich construction; Shell theory; Transverse flexibility; Geometrical nonlinearity; Buckling

1. Introduction

Structural sandwich panels are important elements in many fields of lightweight construction. The classical area of sandwich construction is the field of aerospace engineering. Nevertheless, in the past decades there are strong trends to use sandwich panels also in other technological fields such as in naval and automotive applications or in civil engineering (see e.g. Mouritz et al., 2001). The typical structural sandwich panel is a layered medium consisting of two high-density high-strength face sheets which are adhesively bonded to a thick core made from a low-density material. In most cases, the core consists of a foamed or two-dimensional cellular (honeycomb) material while anisotropic laminae are common as face sheets. Within the principle of sandwich construction, the face sheets carry the tangential and bending loads while the core keeps the face sheets at their desired distance and transmits the transverse normal and shear

* Corresponding author. Tel.: +49-271-740-4642; fax: +49-271-740-2461.
E-mail address: hohe@imr-mail.fb5.uni-siegen.de (J. Hohe).

0020-7683/02/$ - see front matter
PII: S0020-7683(02)00656-X

Nomenclature

A_{ij}, D_{ij}, F_{ij}, H_{ij}	stiffness components
E, G, v	isotropic elasticity constants
K_{ij}, L_{ij}, M_{ij}, N_{ij}	stress resultants
l_i	panel edge lengths
m, n, p, q	number of sine half waves for the different stability modes
q_i	transverse pressure loads
Q_{ij}	reduced stiffness matrix
r_i	radii of curvature
t	layer thicknesses
T	kinetic energy
u_i, $\overset{\circ}{u}_i$	shell mid-plane displacements and initial geometric imperfection
U	strain energy
v_i	three-dimensional shell displacements
w, $\overset{\circ}{w}$	modal amplitude of transverse displacement and initial geometric imperfection
W	work done by external loads
x_i	spatial vector/local Cartesian coordinate system
γ_{ij}	Green–Lagrange strain tensor
$\bar{\gamma}_{ij}$, η_{ij}, ϑ_{ij}, κ_{ij}	shell deformation components
$\delta(\ldots)$	variation of a quantity
ϵ_{ij}	permutation symbol
λ, μ	wavelength parameters
ρ	mass density
τ_{ij}	second Piola–Kirchhoff stress tensor
Φ_i, Ω_i	higher order displacement functions
$(\ldots)^{\mathrm{a}}$	average of quantities related to the top and bottom face sheet
$(\ldots)^{\mathrm{b}}$	quantities related to the bottom face sheet
$(\ldots)^{\mathrm{c}}$	quantities related to the core
$(\ldots)^{\mathrm{d}}$	half difference of quantities related to the top and bottom face sheet
$(\ldots)^{\mathrm{t}}$	quantities related to the top face sheet
$(\widehat{\ldots})$	prescribed quantity
$(\ddot{\ldots})$	second derivative with respect to time

loads. Advantage of this principle of construction is that plates and shells with a rather high-bending stiffness characteristics and an extremely low-specific weight are obtained.

Owing to the thick core consisting of a relatively soft material, the deformation and stability behavior of sandwich structures are essentially different from the corresponding behavior of classical laminated panels and monolayer structures. Especially in structural stability analyses, a different behavior of sandwich structures has to be expected. The transverse flexibility of the core yields an additional instability mode, where buckling of the face sheets into the core region occurs while the overall response of the entire panel might remain stable. In addition to this face wrinkling instability, the standard global instabilities with buckling of the entire panel might also be present.

To account for the specific deformation and buckling behavior, a number of specific plate and shell models for sandwich structures have been developed. Two different types of models can be employed.

Effective single layer theories describe the entire sandwich structure in terms of displacement functions related to one single reference surface. In effective multilayer theories, the individual layers are considered separately. Compatibility is enforced by appropriate interface compatibility constraints.

The main advantage of effective single layer theories is that the total number of unknown field variables and thus also the number of boundary conditions is reduced to a minimum. Recent work on effective single layer sandwich models has been presented by Skvortsov and Bozhevolnaya (2001) as well as by Ferreira et al. (2000). While the first study is restricted to linear elastic material behavior, the latter paper, which is concerned with a finite element implementation, accounts for geometrical and material nonlinearities. An innovative approach to an advanced effective single layer theory for plane sandwich plates has been presented by Barut et al. (2001). This study is based on weighted average displacement functions, where a second and third order approximation is used for the transverse and tangential displacement fields, respectively. The main advantage of this geometrically linear model is that it accounts for the transverse compressibility of the core and satisfies all equilibrium conditions with respect to the transverse stress components in an exact sense.

Disadvantage of effective single layer models is the loss in accuracy due to the simplified displacement representation. Furthermore, it was shown in a finite element analysis by Hao et al. (2000) that effective single layer theories might overestimate the global buckling load of structural sandwich panels. In addition, effective single layer theories are inappropriate, if local or localized effects, such as the face wrinkling instability mode, become significant. These problems are avoided by effective multilayer models where all principal layers are treated separately. Early models of this type are the now classical sandwich membrane models, which assume membrane theory for the face sheets, and pure transverse shear deformation was the only type of deformation considered for the core (Allen, 1969). A number of more sophisticated multilayer sandwich models have been developed during the past decade.

Frostig et al. (1992) provided a geometrically linear multilayer model for straight sandwich beams. This model is based on Kirchhoff theory for the face sheets while no direct displacement assumption is made for the core. By including the transverse shear stress of the core as an independent unknown field variable, a mixed stress–displacement theory is formulated. This approach has been extended to singly curved sandwich beams by Bozhevolnaya and Frostig (1997) and to plane two-dimensional sandwich plates by Frostig (1998). An alternative model for sandwich plates including the transverse normal flexibility of the core has been presented by Lewiński (1991). In his study, the thickness of the core is assumed to be uniform while nonunique transverse displacements in the interior of the core are permitted. Recent theories accounting for the transverse compressibility of the core have been provided by Dawe and Yuan (2001) as well as by Pai and Palazotto (2001). Both of these studies are directed to the analysis of flat sandwich plates in the infinitesimal strain regime. The former study is based on a first and second order displacement expansion for the transverse and tangential displacements, respectively, whereas the latter one uses a second and third order approximation and also accounts for inertia effects. A general, geometrically nonlinear v. Kármán-type theory for doubly curved sandwich shells with transversely incompressible core has been presented by Hause et al. (1998) and Librescu et al. (1997). This theory accounts for initial geometric imperfections and for inertia effects. Surveys on recent developments in the theory and modeling of structural sandwich panels have been provided by Librescu and Hause (2000), Noor et al. (1996) and Vinson (2001).

The necessity to consider the transverse compressibility of the core stems from the fact that this mode of deformation enables the occurrence of the local (face wrinkling) instability as it has already been noted by Frostig et al. (1992) as well as by Starlinger and Rammerstorfer (1992). However, most studies in literature directed to the face wrinkling instability are based on a simplified model where the face sheets are considered as flat panels on an elastic foundation with the material properties of the core (see e.g. Vinson, 1999; Zenkert, 1997). On the other hand, these simplified models might yield inaccurate results, if the buckling load of the global and the local instability are in the same order of magnitude. In this case, coupled buckling modes with different buckling loads arise, where both the global and the face wrinkling instability are

involved. Coupled buckling modes have been observed in a numerical study by Sokolinsky and Frostig (2000) based on the sandwich beam model presented by Frostig et al. (1992). Independently, coupled local and global buckling modes have been observed by da Silva and Santos (1998) as well as by Wadee and Hunt (1998). Again, these studies are restricted to straight sandwich beams.

In order to evaluate the buckling strength and the load carrying capacity of sandwich constructions in a reliable way, a comprehensive structural model that incorporates the transverse normal compressibility effects as well as the geometrical nonlinearities should be developed. This issue motivates the development of the present theory. In the present study, the sandwich shell theory presented by Hause et al. (1998) is extended to sandwich shells with a transversely compressible core. The model adopts the standard Kirchhoff–Love hypothesis for the face sheets, and second and third order expansions of the transverse and tangential displacements for the core, respectively. As a result of the interface compatibility requirements, a total number of 11 unknown displacement functions are finally involved in the general theory. The model accounts for large transverse displacements, initial geometric imperfections, as well as for transverse inertia effects.

The equations of motion and the corresponding boundary conditions for the new sandwich shell model are derived by means of Hamilton's principle. Hence, the derived equations hold irrespectively of the constitutive behavior of the core and the face sheets. In the special case of elastic material behavior of all principal layers, the number of unknown field variables can be reduced to seven. The model is applied to static buckling and postbuckling analyses of simply supported flat and curved sandwich panels. An analytical solution is derived by means of an extended Galerkin scheme. The model is validated by a comparison with theoretical–experimental findings available in the literature. In several examples concerning flat and curved panels, the potential of the new model towards a reliable determination of their load carrying capacity are demonstrated.

2. General theory

2.1. Basic assumptions

Consider a structural sandwich panel according to Fig. 1. The entire structure consists of two thin face sheets and a thick core. The two face sheets are assumed to be equal and uniform throughout the entire sandwich structure. The face sheet thickness is denoted by t^{f} while t^{c} is the core thickness. In general, the core thickness is much larger than the face sheet thickness, however, no specific limiting conditions will be derived from this assumption. Thus, all subsequent considerations hold also for thin cores. Similar to the

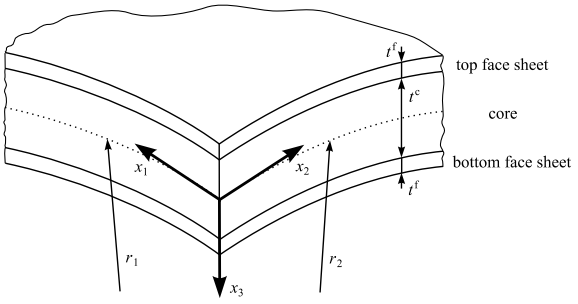

Fig. 1. Structural sandwich panel.

face sheets, the core is assumed to be uniform throughout the entire panel. The bond between the individual layers is considered perfect in the present study.

For the analysis, a local Cartesian coordinate system x_i is defined, where x_1 and x_2 are associated with the global mid-surface of the panel, while x_3 defines the downward normal direction. Thus, the global mid-surface of the panel is employed as the shell reference surface. The sandwich panel is considered doubly curved. The local radii of the curvature in the local x_1–x_3- and the x_2–x_3-planes are denoted by r_1 and r_2, respectively. It is assumed that the radii of curvature are large compared to the core and face sheet thicknesses i.e. $r_1, r_2 \gg t^c, t^f$. Thus the principles of shallow shell theory apply.

Since the tangential stiffness of structural sandwich panels is generally large, it is assumed that the tangential deformation remains small. Contrary, large deflections might occur in the transverse direction. During the deformation, the face sheets are assumed incompressible with respect to the transverse direction while the core, due to its large thickness and weak material, is assumed compressible. Consistent with the assumption of small tangential and large transverse deflections, only transverse inertia effects are considered, whereas all tangential and rotatory inertia effects are discarded.

No specific type of material behavior for either the core layer or the face sheets is specified at this point. However, since within the principle of sandwich construction, the face sheets have to carry the tangential loads and since their tangential stiffness is in general much larger than the tangential stiffness of the core, the work done by the tangential stresses of the core will be neglected. This restriction is consistent with the assumption of the weak core sandwich structures that is adopted for the present study.

2.2. Shell kinematics

As usual in the theory of thin walled structures, the displacement field of the structure is expressed as a power series with respect to the transverse coordinate x_3. In this context, the three principal layers are treated separately. Due to the low thickness of the face sheets, the standard Kirchhoff assumptions are applied to the face sheets. Thus, the displacement fields v_i^t and v_i^b for the top and bottom face sheets in the present problem are given by

$$v_1^t = u_1^a + u_1^d - \left(x_3 + \frac{t^c + t^f}{2}\right) u_{3,1}^a - \left(x_3 + \frac{t^c + t^f}{2}\right) u_{3,1}^d \tag{1}$$

$$v_2^t = u_2^a + u_2^d - \left(x_3 + \frac{t^c + t^f}{2}\right) u_{3,2}^a - \left(x_3 + \frac{t^c + t^f}{2}\right) u_{3,2}^d \tag{2}$$

$$v_3^t = u_3^a + u_3^d \tag{3}$$

and

$$v_1^b = u_1^a - u_1^d - \left(x_3 - \frac{t^c + t^f}{2}\right) u_{3,1}^a + \left(x_3 - \frac{t^c + t^f}{2}\right) u_{3,1}^d \tag{4}$$

$$v_2^b = u_2^a - u_2^d - \left(x_3 - \frac{t^c + t^f}{2}\right) u_{3,2}^a + \left(x_3 - \frac{t^c + t^f}{2}\right) u_{3,2}^d \tag{5}$$

$$v_3^b = u_3^a - u_3^d \tag{6}$$

where the displacement functions

$$u_i^a = \frac{1}{2}\left(u_i^t + u_i^b\right) \tag{7}$$

$$u_i^{\mathrm{d}} = \frac{1}{2}\left(u_i^{\mathrm{t}} - u_i^{\mathrm{b}}\right) \tag{8}$$

represent the average and the half difference of the face sheet mid-surface displacements u_i^{t} and u_i^{b}, respectively. It is implicitly understood, that the three-dimensional displacements v_i^{t} and v_i^{b} depend on all three components x_i of the spatial position vector while the mid-surface displacement functions u_α^{t} and u_α^{b} (and thus u_α^{a} and u_α^{d}) depend solely on the spatial position x_α within the shell reference surface. As usual, Latin indices run over the range 1, 2, 3 while Greek indices run over the range 1, 2. In addition, all displacement functions depend on time. For convenience, the dependences are not indicated explicitly throughout this paper.

Owing to the large core thickness t^{c}, a higher-order expansion has to be used for a proper representation of the core displacement field. Therefore, the tangential displacements are expressed by a third order power series expansion with respect to the thickness direction, while a second order expansion is used for the transverse displacement. Barut et al. (2001) have introduced the naming convention $\{3,2\}$-order theory for this type of approach. Since the displacement field associated with the core has to satisfy the continuity requirements at the face sheet interfaces, the displacement components of the core are obtained in the form

$$v_1^{\mathrm{c}} = u_1^{\mathrm{a}} - \frac{t^{\mathrm{f}}}{2}u_{3,1}^{\mathrm{d}} - \frac{2x_3}{t^{\mathrm{c}}}u_1^{\mathrm{d}} + \frac{t^{\mathrm{f}}}{t^{\mathrm{c}}}x_3 u_{3,1}^{\mathrm{a}} + \left(\frac{4(x_3)^2}{(t^{\mathrm{c}})^2} - 1\right)\Phi_1^{\mathrm{c}} + 2\left(\frac{4(x_3)^2}{(t^{\mathrm{c}})^2} - 1\right)x_3\Omega_1^{\mathrm{c}} \tag{9}$$

$$v_2^{\mathrm{c}} = u_2^{\mathrm{a}} - \frac{t^{\mathrm{f}}}{2}u_{3,2}^{\mathrm{d}} - \frac{2x_3}{t^{\mathrm{c}}}u_2^{\mathrm{d}} + \frac{t^{\mathrm{f}}}{t^{\mathrm{c}}}x_3 u_{3,2}^{\mathrm{a}} + \left(\frac{4(x_3)^2}{(t^{\mathrm{c}})^2} - 1\right)\Phi_2^{\mathrm{c}} + 2\left(\frac{4(x_3)^2}{(t^{\mathrm{c}})^2} - 1\right)x_3\Omega_2^{\mathrm{c}} \tag{10}$$

$$v_3^{\mathrm{c}} = u_3^{\mathrm{a}} - \frac{2x_3}{t^{\mathrm{c}}}u_3^{\mathrm{d}} + \left(\frac{4(x_3)^2}{(t^{\mathrm{c}})^2} - 1\right)\Phi_3^{\mathrm{c}} \tag{11}$$

where Φ_i^{c} and $\Omega_\alpha^{\mathrm{c}}$ are additional displacement functions describing the warping of the core. Similar to the previously introduced displacement functions u_i^{a} and u_i^{d}, the displacement functions Φ_i^{c} and $\Omega_\alpha^{\mathrm{c}}$ depend on the spatial position x_α within the reference surface as well as on time.

In Eq. (11), the second (u_3^{d}-dependent) term captures the transverse compressibility of the core. This term is necessary to account for an independent transverse displacement of the top and bottom face sheets. The last term provides the possibility of an additional transverse warping of the core. Since the power series expansion (11) of the transverse core displacements is of the second order, a third order expansion of the form (9) and (10) has to be used for the tangential displacements.

In addition to the load-dependent displacement functions u_i^{a}, u_i^{d}, Φ_i^{c} and $\Omega_\alpha^{\mathrm{c}}$ in Eqs. (1)–(6) and (9)–(11), a stress-free initial geometric imperfection

$$\overset{\circ}{v}{}_3^{\mathrm{t}} = \overset{\circ}{u}{}_3^{\mathrm{a}} + \overset{\circ}{u}{}_3^{\mathrm{d}} \tag{12}$$

$$\overset{\circ}{v}{}_3^{\mathrm{b}} = \overset{\circ}{u}{}_3^{\mathrm{a}} - \overset{\circ}{u}{}_3^{\mathrm{d}} \tag{13}$$

$$\overset{\circ}{v}{}_3^{\mathrm{c}} = \overset{\circ}{u}{}_3^{\mathrm{a}} - \frac{2x_3}{t^{\mathrm{c}}}\overset{\circ}{u}{}_3^{\mathrm{d}} \tag{14}$$

with respect to the transverse direction is introduced which remains constant during the deformation process. In comparison to the load-dependent displacements, the geometric imperfections are assumed small. Contrary to studies concerned with transversely incompressible panels and monolayer structures (see e.g. Hause et al., 1998), in the present analysis the geometric imperfection of the core has to depend on the

transverse coordinate x_3 in order to ensure compatibility of the transverse displacements across the contiguous surfaces between the compressible core and the face sheets. The total displacement field is given by the sum of the load-dependent displacement field and the initial geometric imperfection. Due to the basic assumption that only the transverse deflections might become large, only stability modes with respect to these displacements might occur. Therefore, only imperfections with respect to the transverse direction are considered.

The deformation of the sandwich shell will be expressed in terms of the Green–Lagrange strain tensor. Due to the basic assumption that only the transverse load-dependent displacements according to Eqs. (3), (6) and (11) might become large while the tangential deflections as well as the initial geometric imperfection are assumed to remain small, only the nonlinear expressions with respect to transverse displacements are kept in the strain-displacement relations while all other nonlinear terms are discarded (Librescu and Chang, 1993). Under the conditions of shallow shell theory, the components of the Green–Lagrange strain tensor for the individual layers read

$$\gamma_{11} = v_{1,1} - \frac{1}{r_1} v_3 + \frac{1}{2}(v_{3,1})^2 + v_{3,1}\overset{\circ}{v}_{3,1} \tag{15}$$

$$\gamma_{22} = v_{2,2} - \frac{1}{r_2} v_3 + \frac{1}{2}(v_{3,2})^2 + v_{3,2}\overset{\circ}{v}_{3,2} \tag{16}$$

$$\gamma_{33} = v_{3,3} + \frac{1}{2}(v_{3,3})^2 + v_{3,3}\overset{\circ}{v}_{3,3} \tag{17}$$

$$\gamma_{23} = \frac{1}{2}(v_{2,3} + v_{3,2}) + \frac{1}{2} v_{3,2} v_{3,3} + \frac{1}{2} v_{3,2}\overset{\circ}{v}_{3,3} + \frac{1}{2}\overset{\circ}{v}_{3,2} v_{3,3} \tag{18}$$

$$\gamma_{13} = \frac{1}{2}(v_{1,3} + v_{3,1}) + \frac{1}{2} v_{3,1} v_{3,3} + \frac{1}{2} v_{3,1}\overset{\circ}{v}_{3,3} + \frac{1}{2}\overset{\circ}{v}_{3,1} v_{3,3} \tag{19}$$

$$\gamma_{12} = \frac{1}{2}(v_{1,2} + v_{2,1}) + \frac{1}{2} v_{3,1} v_{3,2} + \frac{1}{2} v_{3,1}\overset{\circ}{v}_{3,2} + \frac{1}{2}\overset{\circ}{v}_{3,1} v_{3,2} \tag{20}$$

where the radii of curvature r_α for the individual layers are approximated by the radii of the global mid-surface. Eqs. (15)–(20) constitute a sandwich shell theory of the v. Kármán type for infinitesimal strains and moderately large rotations.

Substituting the displacement components according to Eqs. (1)–(6) and (9)–(11) into the nonlinear kinematic equations (15)–(20) yields the components of the Green–Lagrange strain tensor for the individual layers of the sandwich panel. For the top and bottom face sheets, the relations

$$\gamma^{\mathrm{t}}_{\alpha\beta} = \bar{\gamma}^{\mathrm{a}}_{\alpha\beta} + \bar{\gamma}^{\mathrm{d}}_{\alpha\beta} + \left(x_3 + \frac{t^{\mathrm{c}} + t^{\mathrm{f}}}{2}\right)\kappa^{\mathrm{a}}_{\alpha\beta} + \left(x_3 + \frac{t^{\mathrm{c}} + t^{\mathrm{f}}}{2}\right)\kappa^{\mathrm{d}}_{\alpha\beta} \tag{21}$$

$$\gamma^{\mathrm{b}}_{\alpha\beta} = \bar{\gamma}^{\mathrm{a}}_{\alpha\beta} - \bar{\gamma}^{\mathrm{d}}_{\alpha\beta} + \left(x_3 + \frac{t^{\mathrm{c}} + t^{\mathrm{f}}}{2}\right)\kappa^{\mathrm{a}}_{\alpha\beta} - \left(x_3 + \frac{t^{\mathrm{c}} + t^{\mathrm{f}}}{2}\right)\kappa^{\mathrm{d}}_{\alpha\beta} \tag{22}$$

are obtained, where

$$\bar{\gamma}^{\mathrm{a}}_{\alpha\beta} = \frac{1}{2}\left(\bar{\gamma}^{\mathrm{t}}_{\alpha\beta} + \bar{\gamma}^{\mathrm{b}}_{\alpha\beta}\right) \tag{23}$$

$$\bar{\gamma}^{\mathrm{d}}_{\alpha\beta} = \frac{1}{2}\left(\bar{\gamma}^{\mathrm{t}}_{\alpha\beta} - \bar{\gamma}^{\mathrm{b}}_{\alpha\beta}\right) \tag{24}$$

are the average and the half difference of the membrane strains $\bar{\gamma}^{\mathrm{t}}_{\alpha\beta}$ and $\bar{\gamma}^{\mathrm{b}}_{\alpha\beta}$ for the top and bottom face sheet respectively. The quantities

$$\kappa^{\mathrm{a}}_{\alpha\beta} = \frac{1}{2}\left(\kappa^{\mathrm{t}}_{\alpha\beta} + \kappa^{\mathrm{b}}_{\alpha\beta}\right) \tag{25}$$

$$\kappa^{\mathrm{d}}_{\alpha\beta} = \frac{1}{2}\left(\kappa^{\mathrm{t}}_{\alpha\beta} - \kappa^{\mathrm{b}}_{\alpha\beta}\right) \tag{26}$$

are the average and the half difference of the bending strains $\kappa^{\mathrm{t}}_{\alpha\beta}$ and $\kappa^{\mathrm{b}}_{\alpha\beta}$ for the two face sheets. Explicit expressions for the face sheet membrane and bending strains in terms of the displacement functions u^{a}_i and u^{d}_i are given in Appendix A. Owing to the adoption of the Kirchhoff–Love hypothesis, the transverse strain components γ^{t}_{i3} and γ^{b}_{i3} for the top and bottom face sheets vanish identically.

Due to the higher-order displacement representation for the core, more complex expressions for the related components of the Green–Lagrange strain tensor are obtained. The transverse core strain components take the form

$$\gamma^{\mathrm{c}}_{i3} = \bar{\gamma}^{\mathrm{c}}_{i3} + x_3\kappa^{\mathrm{c}}_{i3} + \left((x_3)^2 - \frac{(t^{\mathrm{c}})^2}{4}\right)\eta_{i3} + \left((x_3)^2 - \frac{(t^{\mathrm{c}})^2}{4}\right)x_3\vartheta_{i3} \tag{27}$$

where $\bar{\gamma}^{\mathrm{c}}_{i3}$ and κ_{i3} are the membrane and the bending strain, respectively, for the core whereas η^{c}_{i3} and $\vartheta^{\mathrm{c}}_{i3}$ are higher-order strains resulting from the higher-order core displacements. Explicit expressions for the core strain components are given in Appendix A. Owing to the adoption of the weak core concept, the tangential strain components $\gamma^{\mathrm{c}}_{\alpha\beta}$ for the core are not involved in the subsequent developments and therefore they are not provided in explicit form.

In conjunction with a specific constitutive equation (which is not adopted so far), and with the equations of motion to be determined in Section 2.3, it will be shown that the strain components $\bar{\gamma}^{\mathrm{c}}_{i3}$, κ_{i3}, η^{c}_{i3} and $\vartheta^{\mathrm{c}}_{\alpha 3}$ are not independent from each other. In this case, four of the displacement functions of the core can be eliminated from the system, resulting in the vanishing of the antisymmetric terms in Eq. (27).

2.3. Equations of motion and boundary conditions

The equations of motion have to be consistent with the assumptions made during the determination of the kinematic relations (23), (24) and (27). Consistent equations of motion as well as the corresponding boundary conditions can be obtained in a natural manner from Hamilton's principle

$$\int_{t^0}^{t^1} (\delta U - \delta W - \delta T)\mathrm{d}t = 0 \tag{28}$$

where δU, δW and δT are the variations of the strain energy, of the work done by the external loads and of the kinetic energy, respectively, in case of a virtual displacement δu^{a}_i, δu^{d}_i, $\delta \Phi^{\mathrm{c}}_3$ and $\delta \Omega^{\mathrm{c}}_\alpha$ of the entire sandwich structure during the time interval $[t^0, t^1]$.

Under the basic assumption that the work done by the tangential stresses of the core is negligible, the variation of the strain energy is expressed as

$$\delta U = \int_A \left(\int_{-t^{\mathrm{f}}-\frac{t^{\mathrm{c}}}{2}}^{-\frac{t^{\mathrm{c}}}{2}} \tau^{\mathrm{t}}_{\alpha\beta}\delta\gamma^{\mathrm{t}}_{\alpha\beta}\,\mathrm{d}x_3 + \int_{-\frac{t^{\mathrm{c}}}{2}}^{\frac{t^{\mathrm{c}}}{2}} \tau^{\mathrm{c}}_{i3}\delta\gamma^{\mathrm{c}}_{i3}\,\mathrm{d}x_3 + \int_{\frac{t^{\mathrm{c}}}{2}}^{\frac{t^{\mathrm{c}}}{2}+t^{\mathrm{f}}} \tau^{\mathrm{b}}_{\alpha\beta}\delta\gamma^{\mathrm{b}}_{\alpha\beta}\,\mathrm{d}x_3 \right)\mathrm{d}A \tag{29}$$

where τ_{ij} are the components of the second Piola–Kirchhoff stress tensor, while A denotes the area of the sandwich panel under consideration.

With respect to the variation δW of the work done by the external loads, all tangential distributed loads on the area A of the sandwich panel are neglected. Along the external boundary of the sandwich panel, it is assumed that all prescribed tangential loads are transmitted by the face sheets while all prescribed transverse loads will are carried by the core. A local coordinate system is introduced where x_n and x_t are the normal and tangential directions on the external boundary, respectively. Thus, the variation of the work done by the external loads is given by

$$\delta W = \int_A \left(\hat{q}_3^{\mathrm{t}} \delta u_3^{\mathrm{t}} + \hat{q}_3^{\mathrm{b}} \delta u_3^{\mathrm{b}} \right) \mathrm{d}A + \int_{x_t} \left(\int_{-t^{\mathrm{f}}-\frac{t^{\mathrm{c}}}{2}}^{-\frac{t^{\mathrm{c}}}{2}} \hat{\tau}_{n\alpha^*}^{\mathrm{t}} \delta v_{\alpha^*}^{\mathrm{t}} \, \mathrm{d}x_3 + \int_{-\frac{t^{\mathrm{c}}}{2}}^{\frac{t^{\mathrm{c}}}{2}} \hat{\tau}_{n3}^{\mathrm{c}} \delta v_3^{\mathrm{c}} \, \mathrm{d}x_3 + \int_{\frac{t^{\mathrm{c}}}{2}}^{\frac{t^{\mathrm{c}}}{2}+t^{\mathrm{f}}} \hat{\tau}_{n\alpha^*}^{\mathrm{b}} \delta v_{\alpha^*}^{\mathrm{b}} \, \mathrm{d}x_3 \right) \mathrm{d}x_t \tag{30}$$

where $\hat{q}_3^{\mathrm{t}}$ and $\hat{q}_3^{\mathrm{b}}$ are the distributed loads on the top and bottom face sheet respectively while $\hat{\tau}_{ij}$ denote the prescribed stresses along the external boundary and $\alpha^* = n, t$.

If all tangential and rotatory inertia effects are discarded, the variation of the kinetic energy of the sandwich panel is given by

$$\int_{t^0}^{t^1} \delta T \, \mathrm{d}t = \int_{t^0}^{t^1} \int_A \left(\int_{-t^{\mathrm{f}}-\frac{t^{\mathrm{c}}}{2}}^{-\frac{t^{\mathrm{c}}}{2}} - \rho^{\mathrm{f}} \ddot{v}_3^{\mathrm{t}} \delta v_3^{\mathrm{t}} \, \mathrm{d}x_3 + \int_{-\frac{t^{\mathrm{c}}}{2}}^{\frac{t^{\mathrm{c}}}{2}} - \rho^{\mathrm{c}} \ddot{v}_3^{\mathrm{c}} \delta v_3^{\mathrm{c}} \, \mathrm{d}x_3 + \int_{\frac{t^{\mathrm{c}}}{2}}^{\frac{t^{\mathrm{c}}}{2}+t^{\mathrm{f}}} - \rho^{\mathrm{f}} \ddot{v}_3^{\mathrm{b}} \delta v_3^{\mathrm{b}} \, \mathrm{d}x_3 \right) \mathrm{d}A \, \mathrm{d}t \tag{31}$$

where ρ^{c} and ρ^{f} are the mass densities of the core and of the face sheets, respectively, and $\ddot{v}_3$ denotes the transverse acceleration.

In order to determine the nonlinear equations of motion and the corresponding boundary conditions, the variations $\gamma_{\alpha\beta}^{\mathrm{t}}$, $\gamma_{\alpha\beta}^{\mathrm{b}}$ and γ_{i3}^{c} are derived from relations (23)–(27) for the corresponding strain components and substituted into Eq. (29). Subsequently, the stress resultants and stress couples

$$\left\{ N_{\alpha\beta}^{\mathrm{t}}, M_{\alpha\beta}^{\mathrm{t}} \right\} = \int_{-t^{\mathrm{f}}-\frac{t^{\mathrm{c}}}{2}}^{-\frac{t^{\mathrm{c}}}{2}} \tau_{\alpha\beta}^{\mathrm{t}} \left\{ 1, \left(x_3 + \frac{t^{\mathrm{c}} + t^{\mathrm{f}}}{2} \right) \right\} \mathrm{d}x_3 \tag{32}$$

$$\left\{ N_{\alpha\beta}^{\mathrm{b}}, M_{\alpha\beta}^{\mathrm{b}} \right\} = \int_{\frac{t^{\mathrm{c}}}{2}}^{t^{\mathrm{f}}+\frac{t^{\mathrm{c}}}{2}} \tau_{\alpha\beta}^{\mathrm{t}} \left\{ 1, \left(x_3 - \frac{t^{\mathrm{c}} + t^{\mathrm{f}}}{2} \right) \right\} \mathrm{d}x_3 \tag{33}$$

$$\left\{ N_{i3}^{\mathrm{c}}, M_{i3}^{\mathrm{c}}, L_{i3}^{\mathrm{c}}, K_{i3}^{\mathrm{c}} \right\} = \int_{-\frac{t^{\mathrm{c}}}{2}}^{\frac{t^{\mathrm{c}}}{2}} \tau_{i3}^{\mathrm{t}} \left\{ 1, x_3, \left((x_3)^2 - \frac{(t^{\mathrm{c}})^2}{2} \right), \left((x_3)^2 - \frac{(t^{\mathrm{c}})^2}{2} \right) x_3 \right\} \mathrm{d}x_3 \tag{34}$$

are introduced to replace the stress components τ_{ij} in Eqs. (29)–(31). For convenience, alternative average and difference stress resultants according to

$$N_{\alpha\beta}^{\mathrm{a}} = \frac{1}{2} \left(N_{\alpha\beta}^{\mathrm{t}} + N_{\alpha\beta}^{\mathrm{b}} \right) \tag{35}$$

$$N_{\alpha\beta}^{\mathrm{d}} = \frac{1}{2} \left(N_{\alpha\beta}^{\mathrm{t}} - N_{\alpha\beta}^{\mathrm{b}} \right) \tag{36}$$

$$M_{\alpha\beta}^{\mathrm{a}} = \frac{1}{2} \left(M_{\alpha\beta}^{\mathrm{t}} + M_{\alpha\beta}^{\mathrm{b}} \right) \tag{37}$$

$$M_{\alpha\beta}^{\mathrm{d}} = \frac{1}{2} \left(M_{\alpha\beta}^{\mathrm{t}} - M_{\alpha\beta}^{\mathrm{b}} \right) \tag{38}$$

are defined for the top and bottom face sheets.

By substituting Eqs. (29)–(31) in conjunction with the two-dimensional stress measures Eqs. (32)–(38) into Hamilton's principle (28), collecting the coefficients of each of the virtual displacements, and integrating by parts whenever necessary as to relieve the virtual displacements of any differentiation, a single homogeneous linear equation for the virtual displacements δu_i^{a}, δu_i^{d}, $\delta \Phi_i^{\mathrm{c}}$ and $\delta \Omega_\alpha^{\mathrm{a}}$ is obtained. Since the virtual displacements are independent and arbitrary, the corresponding coefficients in this homogeneous equation must vanish independently. Thus, the nonlinear equations of motion

$$0 = N^{\mathrm{a}}_{11,1} + N^{\mathrm{a}}_{12,2} \tag{39}$$

$$0 = N^{\mathrm{a}}_{12,1} + N^{\mathrm{a}}_{22,2} \tag{40}$$

$$0 = N^{\mathrm{d}}_{11,1} + N^{\mathrm{d}}_{12,2} + \frac{1}{t^{\mathrm{c}}} N^{\mathrm{c}}_{13} \tag{41}$$

$$0 = N^{\mathrm{d}}_{12,1} + N^{\mathrm{d}}_{22,2} + \frac{1}{t^{\mathrm{c}}} N^{\mathrm{c}}_{23} \tag{42}$$

$$0 = M^{\mathrm{c}}_{13} \tag{43}$$

$$0 = M^{\mathrm{c}}_{23} \tag{44}$$

$$0 = N^{\mathrm{c}}_{13} + \frac{6}{(t^{\mathrm{c}})^2} L^{\mathrm{c}}_{13} \tag{45}$$

$$0 = N^{\mathrm{c}}_{23} + \frac{6}{(t^{\mathrm{c}})^2} L^{\mathrm{c}}_{23} \tag{46}$$

$$\begin{aligned} 0 = {} & \left(u^{\mathrm{a}}_{3,11} + \mathring{u}^{\mathrm{a}}_{3,11} + \frac{1}{r_1}\right) N^{\mathrm{a}}_{11} + 2\left(u^{\mathrm{a}}_{3,12} + \mathring{u}^{\mathrm{a}}_{3,12}\right) N^{\mathrm{a}}_{12} + \left(u^{\mathrm{a}}_{3,22} + \mathring{u}^{\mathrm{a}}_{3,22} + \frac{1}{r_2}\right) N^{\mathrm{a}}_{22} + M^{\mathrm{a}}_{11,11} + 2M^{\mathrm{a}}_{12,12} + M^{\mathrm{a}}_{22,22} \\ & + \left(u^{\mathrm{d}}_{3,11} + \mathring{u}^{\mathrm{d}}_{3,11}\right) N^{\mathrm{d}}_{11} + 2\left(u^{\mathrm{d}}_{3,12} + \mathring{u}^{\mathrm{d}}_{3,12}\right) N^{\mathrm{d}}_{12} + \left(u^{\mathrm{d}}_{3,22} + \mathring{u}^{\mathrm{d}}_{3,22}\right) N^{\mathrm{d}}_{22} + \frac{1}{t^{\mathrm{c}}}\left(\frac{t^{\mathrm{c}} + t^{\mathrm{f}}}{2} - u^{\mathrm{d}}_3 - \mathring{u}^{\mathrm{d}}_3\right)\left(N^{\mathrm{c}}_{13,1} + N^{\mathrm{c}}_{23,2}\right) \\ & - \frac{2}{t^{\mathrm{c}}}\left(u^{\mathrm{d}}_{3,1} + \mathring{u}^{\mathrm{d}}_{3,1}\right) N^{\mathrm{c}}_{13} - \frac{2}{t^{\mathrm{c}}}\left(u^{\mathrm{d}}_{3,2} + \mathring{u}^{\mathrm{d}}_{3,2}\right) N^{\mathrm{c}}_{23} + \hat{q}^{\mathrm{a}}_3 - \left(m^{\mathrm{f}} + \frac{1}{2} m^{\mathrm{c}}\right) \ddot{u}^{\mathrm{a}}_3 + \frac{1}{3} m^{\mathrm{c}} \ddot{\Phi}^{\mathrm{c}}_3 \end{aligned} \tag{47}$$

$$\begin{aligned} 0 = {} & \left(u^{\mathrm{a}}_{3,11} + \mathring{u}^{\mathrm{a}}_{3,11} + \frac{1}{r_1}\right) N^{\mathrm{d}}_{11} + 2\left(u^{\mathrm{a}}_{3,12} + \mathring{u}^{\mathrm{a}}_{3,12}\right) N^{\mathrm{d}}_{12} + \left(u^{\mathrm{a}}_{3,22} + \mathring{u}^{\mathrm{a}}_{3,22} + \frac{1}{r_2}\right) N^{\mathrm{d}}_{22} + M^{\mathrm{d}}_{11,11} + 2M^{\mathrm{d}}_{12,12} + M^{\mathrm{d}}_{22,22} \\ & + \left(u^{\mathrm{d}}_{3,11} + \mathring{u}^{\mathrm{d}}_{3,11}\right) N^{\mathrm{a}}_{11} + 2\left(u^{\mathrm{d}}_{3,12} + \mathring{u}^{\mathrm{d}}_{3,12}\right) N^{\mathrm{a}}_{12} + \left(u^{\mathrm{d}}_{3,22} + \mathring{u}^{\mathrm{d}}_{3,22}\right) N^{\mathrm{a}}_{22} + \frac{2}{t^{\mathrm{c}}}\left(\frac{t^{\mathrm{c}}}{2} - u^{\mathrm{d}}_3 - \mathring{u}^{\mathrm{d}}_3\right) N^{\mathrm{c}}_{33} \\ & - \frac{2}{3t^{\mathrm{c}}} \Phi^{\mathrm{c}}_3 \left(N^{\mathrm{c}}_{13,1} + N^{\mathrm{c}}_{23,2}\right) - \frac{4}{3t^{\mathrm{c}}} \Phi^{\mathrm{c}}_{3,1} N^{\mathrm{c}}_{13} - \frac{4}{3t^{\mathrm{c}}} \Phi^{\mathrm{c}}_{3,2} N^{\mathrm{c}}_{23} - \frac{8}{(t^{\mathrm{c}})^3} \Phi^{\mathrm{c}}_3 M^{\mathrm{c}}_{33} + \hat{q}^{\mathrm{d}}_3 - \left(m^{\mathrm{f}} + \frac{1}{6} m^{\mathrm{c}}\right) \ddot{u}^{\mathrm{d}}_3 \end{aligned} \tag{48}$$

$$\begin{aligned} 0 = {} & -\frac{8}{(t^{\mathrm{c}})^2} \Phi^{\mathrm{c}}_3 N^{\mathrm{c}}_{33} + \frac{4}{3t^{\mathrm{c}}}\left(u^{\mathrm{d}}_{3,1} + \mathring{u}^{\mathrm{d}}_{3,1}\right) N^{\mathrm{c}}_{13} + \frac{4}{3t^{\mathrm{c}}}\left(u^{\mathrm{d}}_{3,2} + \mathring{u}^{\mathrm{d}}_{3,2}\right) N^{\mathrm{c}}_{23} - \frac{2}{3t^{\mathrm{c}}}\left(\frac{t^{\mathrm{c}}}{2} - u^{\mathrm{d}}_3 - \mathring{u}^{\mathrm{d}}_3\right)\left(N^{\mathrm{c}}_{13,1} + N^{\mathrm{c}}_{23,2}\right) \\ & - \frac{8}{(t^{\mathrm{c}})^3}\left(\frac{t^{\mathrm{c}}}{2} - u^{\mathrm{d}}_3 - \mathring{u}^{\mathrm{d}}_3\right) M^{\mathrm{c}}_{33} - \frac{32}{(t^{\mathrm{c}})^4} \Phi^{\mathrm{c}}_3 L^{\mathrm{c}}_{33} + \frac{16}{(t^{\mathrm{c}})^4} \Phi^{\mathrm{c}}_3 \left(K^{\mathrm{c}}_{13,1} + K^{\mathrm{c}}_{23,2}\right) + \frac{1}{3} m^{\mathrm{c}} \ddot{u}^{\mathrm{a}}_3 - \frac{4}{15} m^{\mathrm{c}} \ddot{\Phi}^{\mathrm{c}}_3 \end{aligned} \tag{49}$$

with

$$\hat{q}_3^{\mathrm{a}} = \frac{1}{2}\left(\hat{q}_3^{\mathrm{t}} + \hat{q}_3^{\mathrm{b}}\right) \tag{50}$$

$$\hat{q}_3^{\mathrm{d}} = \frac{1}{2}\left(\hat{q}_3^{\mathrm{t}} - \hat{q}_3^{\mathrm{b}}\right) \tag{51}$$

are obtained, where m^{f} and m^{c} are the reduced mass densities for the face sheets and the core, respectively, integrated with respect to the individual layer thickness. As it has to be expected, due to the basic assumption of infinitesimal tangential strains, the first two equations in this system are identical to the equilibrium conditions in membrane theory. The third and fourth equations are also a kind of membrane equations which describe the coupling between the membrane stress resultants of the face sheets and the transverse shear stresses of the core. The fifth to eighth equations constitute a result of the tangential deformation components Φ_α^{c} and $\Omega_\alpha^{\mathrm{c}}$ of the core. Due to the involved kinematic assumptions, these equations are also linear. The last three equations are related to the transverse direction where large deflections are involved. Hence, these equations are nonlinear. Since only the transverse inertia effects are considered, Eqs. (47)–(49) are the only equations containing inertia terms.

The corresponding nonhomogeneous boundary conditions along the external boundaries of the sandwich panel read

$$u_n^{\mathrm{a}} = \hat{u}_n^{\mathrm{a}} \quad \text{or} \quad N_{nn}^{\mathrm{a}} = \widehat{N}_{nn}^{\mathrm{a}} \tag{52}$$

$$u_t^{\mathrm{a}} = \hat{u}_t^{\mathrm{a}} \quad \text{or} \quad N_{nt}^{\mathrm{a}} = \widehat{N}_{nt}^{\mathrm{a}} \tag{53}$$

$$u_n^{\mathrm{d}} = \hat{u}_n^{\mathrm{d}} \quad \text{or} \quad N_{nn}^{\mathrm{d}} = \widehat{N}_{nn}^{\mathrm{d}} \tag{54}$$

$$u_t^{\mathrm{d}} = \hat{u}_t^{\mathrm{d}} \quad \text{or} \quad N_{nt}^{\mathrm{d}} = \widehat{N}_{nt}^{\mathrm{d}} \tag{55}$$

$$u_3^{\mathrm{a}} = \hat{u}_3^{\mathrm{a}} \quad \text{or} \quad \left(u_{3,n}^{\mathrm{a}} + \mathring{u}_{3,n}^{\mathrm{a}}\right)N_{nn}^{\mathrm{a}} + \left(u_{3,t}^{\mathrm{a}} + \mathring{u}_{3,t}^{\mathrm{a}}\right)N_{nt}^{\mathrm{a}} + \left(u_{3,n}^{\mathrm{d}} + \mathring{u}_{3,n}^{\mathrm{d}}\right)N_{nn}^{\mathrm{d}} + \left(u_{3,t}^{\mathrm{d}} + \mathring{u}_{3,t}^{\mathrm{d}}\right)N_{nt}^{\mathrm{d}} + M_{nn,n}^{\mathrm{a}} + 2M_{nt,t}^{\mathrm{a}} + \frac{1}{t^{\mathrm{c}}}\left(\frac{t^{\mathrm{c}} + t^{\mathrm{f}}}{2} - u_3^{\mathrm{d}} - \mathring{u}_3^{\mathrm{d}}\right)N_{n3}^{\mathrm{c}} = \widehat{M}_{nt,t}^{\mathrm{a}} + \frac{1}{2}\widehat{N}_{n3}^{\mathrm{c}} \tag{56}$$

$$u_3^{\mathrm{d}} = \hat{u}_3^{\mathrm{d}} \quad \text{or} \quad \left(u_{3,n}^{\mathrm{a}} + \mathring{u}_{3,n}^{\mathrm{a}}\right)N_{nn}^{\mathrm{d}} + \left(u_{3,t}^{\mathrm{a}} + \mathring{u}_{3,t}^{\mathrm{a}}\right)N_{nt}^{\mathrm{d}} + \left(u_{3,n}^{\mathrm{d}} + \mathring{u}_{3,n}^{\mathrm{d}}\right)N_{nn}^{\mathrm{a}} + \left(u_{3,t}^{\mathrm{d}} + \mathring{u}_{3,t}^{\mathrm{d}}\right)N_{nt}^{\mathrm{a}} + M_{nn,n}^{\mathrm{d}} + 2M_{nt,t}^{\mathrm{d}} - \frac{2}{3t^{\mathrm{c}}}\Phi_3^{\mathrm{c}}N_{n3}^{\mathrm{c}} = \widehat{M}_{nt,t}^{\mathrm{d}} - \frac{1}{t^{\mathrm{c}}}\widehat{M}_{n3}^{\mathrm{c}} \tag{57}$$

$$\Phi_3^{\mathrm{c}} = \hat{\Phi}_3^{\mathrm{c}} \quad \text{or} \quad \frac{2}{t^{\mathrm{c}}}\left(\frac{t^{\mathrm{c}}}{2} - u_3^{\mathrm{d}} - \mathring{u}_3^{\mathrm{d}}\right)N_{n3}^{\mathrm{c}} - \frac{48}{\left(t^{\mathrm{c}}\right)^4}\Phi_3^{\mathrm{c}}K_{n3}^{\mathrm{c}} = \widehat{N}_{n3}^{\mathrm{c}} \tag{58}$$

$$u_{3,n}^{\mathrm{a}} = \hat{u}_{3,n}^{\mathrm{a}} \quad \text{or} \quad M_{nn}^{\mathrm{a}} = \widehat{M}_{nn}^{\mathrm{a}} \tag{59}$$

$$u_{3,n}^{\mathrm{d}} = \hat{u}_{3,n}^{\mathrm{d}} \quad \text{or} \quad M_{nn}^{\mathrm{d}} = \widehat{M}_{nn}^{\mathrm{d}}. \tag{60}$$

Thus, along each edge of the panel, either the tangential displacements or the corresponding stress resultant has to be specified for both face sheets in terms of the average and the difference according to Eqs. (7) and (8) or (35) and (36). In addition, either the rotations with respect to the longitudinal direction of

each edge or the corresponding stress couples have to be prescribed. With respect to the transverse direction, the displacement functions u_3^{a}, u_3^{d} and Φ_3^{c} can be specified along the panel edges. In the case of nonvanishing transverse edge displacements, nonlinear boundary conditions apply due to the assumption of large transverse deflections. Since a total of nine independent boundary conditions have to be satisfied along each edge of the panel, the governing system is of the 18th order.

Note that so far no specific type of material behavior has been considered. Thus, the nonlinear equations of motion (39)–(49) as well as the corresponding boundary conditions (52)–(60) hold irrespectively of the constitutive equations for the core and the face sheets as long as the basic assumptions from Section 2.1 are satisfied.

2.4. Compatibility equation

The first two equilibrium conditions (39) and (40) are satisfied identically by introduction of an Airy stress function Φ for the average tangential stress resultants $N_{\alpha\beta}^{\mathrm{a}}$ of the top and bottom face sheets. The stress resultants are obtained as the second partial derivatives

$$N_{\alpha\beta}^{\mathrm{a}} = \epsilon_{\alpha\gamma}\epsilon_{\beta\delta}\Phi_{,\gamma\delta} \tag{61}$$

of the Airy function, where $\epsilon_{\alpha\beta}$ denotes the permutation symbol.

Introduction of the Airy stress function implies that Eqs. (39) and (40) are eliminated from the system. On the other hand, with the Airy function Φ, an additional field quantity has been introduced. Therefore, an additional equation is required. This equation can be obtained in form of a compatibility condition for the average tangential membrane strain components $\bar{\gamma}_{\alpha\beta}^{\mathrm{a}}$ similar to the compatibility condition for the strain components in three-dimensional continuum mechanics. For the present sandwich shell theory, the compatibility equation takes the form:

$$\begin{aligned}\bar{\gamma}_{11,22}^{\mathrm{a}} - 2\bar{\gamma}_{12,12}^{\mathrm{a}} + \bar{\gamma}_{22,11}^{\mathrm{a}} = &-\frac{1}{r_1}u_{3,22}^{\mathrm{a}} - \frac{1}{r_2}u_{3,11}^{\mathrm{a}} + (u_{3,12}^{\mathrm{a}})^2 + 2u_{3,12}^{\mathrm{a}}\overset{\circ}{u}{}_{3,12}^{\mathrm{a}} - u_{3,11}^{\mathrm{a}}u_{3,22}^{\mathrm{a}} - \overset{\circ}{u}{}_{3,11}^{\mathrm{a}}u_{3,22}^{\mathrm{a}} \\ &- u_{3,11}^{\mathrm{a}}\overset{\circ}{u}{}_{3,22}^{\mathrm{a}} + (u_{3,12}^{\mathrm{d}})^2 + 2u_{3,12}^{\mathrm{d}}\overset{\circ}{u}{}_{3,12}^{\mathrm{d}} - u_{3,11}^{\mathrm{d}}u_{3,22}^{\mathrm{d}} - \overset{\circ}{u}{}_{3,11}^{\mathrm{d}}u_{3,22}^{\mathrm{d}} - u_{3,11}^{\mathrm{d}}\overset{\circ}{u}{}_{3,22}^{\mathrm{d}}.\end{aligned} \tag{62}$$

Introduction of the Airy stress function Φ according to Eq. (61) and replacement of the two—now obsolete—equilibrium conditions (39) and (40) by the compatibility equation (62), implies a reduction of the governing system in the number of equations by one. Similar as in the standard v. Kármán theory for shallow monolayer shells, the overall problem can be regarded as an tangential and a bending problem, which is coupled via the transverse displacements and via the curvature.

3. Special case: orthotropic elasticity

In Section 2, no specific type of material behavior has been considered. Thus, the nonlinear sandwich shell theory defined by the kinematic equations (1)–(6) and (9)–(11), the equations of motion (41)–(49), the compatibility equation (62) and the corresponding boundary conditions (52)–(60) is valid for all types of material behavior. If the theory is specialized to linear elastic behavior, the governing system of equations can be reduced in the number of unknown displacement functions.

The face sheets are subsequently assumed to consist of orthotropic laminae. If the axes of orthotropy coincide with the axes x_i of the coordinate system and if the lay-up of the face sheets is symmetric with respect to their individual mid-surfaces, the average face sheet stress resultants $N_{\alpha\beta}^{\mathrm{a}}$ and $M_{\alpha\beta}^{\mathrm{a}}$ are related to the average mid-surface strain and curvature components $\bar{\gamma}_{\alpha\beta}^{\mathrm{a}}$ and $\kappa_{\alpha\beta}^{\mathrm{a}}$ of the face sheets by

$$\begin{pmatrix} N_{11}^{a} \\ N_{22}^{a} \\ N_{12}^{a} \end{pmatrix} = \begin{pmatrix} A_{11}^{f} & A_{12}^{f} & 0 \\ & A_{22}^{f} & 0 \\ (\text{Sym.}) & & A_{66}^{f} \end{pmatrix} \begin{pmatrix} \bar{\gamma}_{11}^{a} \\ \bar{\gamma}_{22}^{a} \\ 2\bar{\gamma}_{12}^{a} \end{pmatrix} \tag{63}$$

and

$$\begin{pmatrix} M_{11}^{a} \\ M_{22}^{a} \\ M_{12}^{a} \end{pmatrix} = \begin{pmatrix} D_{11}^{f} & D_{12}^{f} & 0 \\ & D_{22}^{f} & 0 \\ (\text{Sym.}) & & D_{66}^{f} \end{pmatrix} \begin{pmatrix} \kappa_{11}^{a} \\ \kappa_{22}^{a} \\ 2\kappa_{12}^{a} \end{pmatrix}. \tag{64}$$

Similar relations with the same stiffness coefficients A_{ij}^{f} and D_{ij}^{f} relate the half differences $N_{\alpha\beta}^{d}$ and $M_{\alpha\beta}^{d}$ of the face sheet stress resultants to the half differences $\bar{\gamma}_{\alpha\beta}^{d}$ and $\kappa_{\alpha\beta}^{d}$ of the face sheet mid-surface strains and curvature changes. The stiffness components are defined in the usual manner by

$$\left\{A_{ij}^{f}, D_{ij}^{f}\right\} = \int_{-t^{f}-\frac{t^{c}}{2}}^{-\frac{t^{c}}{2}} \left(Q_{ij}^{f} - \frac{Q_{i3}^{f}Q_{j3}^{f}}{Q_{33}^{f}}\right) \left\{1, \left(x_3 + \frac{t^{c}+t^{f}}{2}\right)^{2}\right\} \mathrm{d}x_3 \tag{65}$$

where Q_{ij}^{f} are the components of the reduced stiffness matrix for the face sheets. Explicit expressions for the face sheet strain components $\bar{\gamma}_{\alpha\beta}^{a}$, $\bar{\gamma}_{\alpha\beta}^{d}$, $\kappa_{\alpha\beta}^{a}$ and $\kappa_{\alpha\beta}^{d}$ in terms of the displacement functions u_i^{a}, u_i^{d} and the initial geometric imperfections are provided in Appendix A.

The core is also assumed to be linearly elastic and orthotropic. Again, the axes of orthotropy are assumed to coincide with the coordinate axes x_i. In this case, the stress resultants N_{i3}^{c}, M_{i3}^{c}, L_{i3}^{c} and K_{i3}^{c} are related to the core deformation components $\bar{\gamma}_{i3}^{c}$, κ_{i3}^{c}, η_{i3}^{c} and ϑ_{i3}^{c} according to Appendix A by the relations

$$\begin{pmatrix} N_{33}^{c} \\ N_{23}^{c} \\ N_{13}^{c} \end{pmatrix} = \begin{pmatrix} A_{33}^{c}\bar{\gamma}_{33}^{c} + \left(D_{33}^{c} - \frac{(t^{c})^{2}}{4}A_{33}^{c}\right)\eta_{33}^{c} \\ A_{44}^{c}2\bar{\gamma}_{23}^{c} + \left(D_{44}^{c} - \frac{(t^{c})^{2}}{4}A_{44}^{c}\right)2\eta_{23}^{c} \\ A_{55}^{c}2\bar{\gamma}_{13}^{c} + \left(D_{55}^{c} - \frac{(t^{c})^{2}}{4}A_{55}^{c}\right)2\eta_{13}^{c} \end{pmatrix} \tag{66}$$

$$\begin{pmatrix} M_{33}^{c} \\ M_{23}^{c} \\ M_{13}^{c} \end{pmatrix} = \begin{pmatrix} D_{33}^{c}\kappa_{33}^{c} \\ D_{44}^{c}2\kappa_{23}^{c} + \left(F_{44}^{c} + \frac{(t^{c})^{2}}{4}D_{44}^{c} - \frac{(t^{c})^{4}}{16}A_{44}^{c}\right)2\vartheta_{23}^{c} \\ D_{55}^{c}2\kappa_{13}^{c} + \left(F_{55}^{c} + \frac{(t^{c})^{2}}{4}D_{55}^{c} - \frac{(t^{c})^{4}}{16}A_{55}^{c}\right)2\vartheta_{13}^{c} \end{pmatrix} \tag{67}$$

$$\begin{pmatrix} L_{33}^{c} \\ L_{23}^{c} \\ L_{13}^{c} \end{pmatrix} = \begin{pmatrix} \left(D_{33}^{c} - \frac{(t^{c})^{2}}{4}A_{33}^{c}\right)\bar{\gamma}_{33}^{c} + F_{33}^{c}\eta_{33}^{c} \\ \left(D_{44}^{c} - \frac{(t^{c})^{2}}{4}A_{44}^{c}\right)2\bar{\gamma}_{23}^{c} + F_{44}^{c}2\eta_{23}^{c} \\ \left(D_{55}^{c} - \frac{(t^{c})^{2}}{4}A_{55}^{c}\right)2\bar{\gamma}_{13}^{c} + F_{55}^{c}2\eta_{13}^{c} \end{pmatrix} \tag{68}$$

$$\begin{pmatrix} K_{23}^{c} \\ K_{13}^{c} \end{pmatrix} = \begin{pmatrix} \left(F_{44}^{c} + \frac{(t^{c})^{2}}{4}D_{44}^{c} - \frac{(t^{c})^{4}}{16}A_{44}^{c}\right)2\kappa_{23}^{c} + H_{44}^{c}2\vartheta_{23}^{c} \\ \left(F_{55}^{c} + \frac{(t^{c})^{2}}{4}D_{55}^{c} - \frac{(t^{c})^{4}}{16}A_{55}^{c}\right)2\kappa_{13}^{c} + H_{55}^{c}2\vartheta_{13}^{c} \end{pmatrix} \tag{69}$$

which are obtained by substituting the components γ_{i3}^{c} of the Green–Lagrange strain tensor into the three-dimensional constitutive equation for orthotropic elasticity and a subsequent substitution of the obtained transverse components τ_{i3}^{c} of the second Piola–Kirchhoff stress tensor into relation (34) for the core stress resultants. The core stiffness components are given by

$$\{A^{c}_{(ii)}, D^{c}_{(ii)}, F^{c}_{(ii)}, H^{c}_{(ii)}\} = \int_{-\frac{t^c}{2}}^{\frac{t^c}{2}} Q^{c}_{(ii)} \left\{ 1, (x_3)^2, \left((x_3)^2 - \frac{(t^c)^2}{4} \right)^2, \left((x_3)^2 - \frac{(t^c)^2}{4} \right)^2 (x_3)^2 \right\} \mathrm{d}x_3 \quad i = 3,4,5 \tag{70}$$

where no summation with respect to repeated indices in parentheses has to be performed.

The constitutive relations (66)–(69) can be employed to eliminate four unknown displacement functions from the system: Substituting the core deformation components $\bar{\gamma}^{c}_{i3}$, κ^{c}_{i3}, η^{c}_{i3} and ϑ^{c}_{i3} according to Appendix A into the constitutive equations (66)–(68) yields closed-form expressions for the core stress resultants N^{c}_{i3}, M^{c}_{i3} and L^{c}_{i3}. Substituting the result into the fifth to eighth equation of motion (43)–(46) yields four algebraic equations for the tangential core displacement functions Φ^{c}_{α} and Ω^{c}_{α}. In conjunction with the assumption that the material behavior is uniform with respect to the core thickness so that the reduced stiffness components $Q^{c}_{(ii)}$ do not depend on the transverse direction x_3, the result reads

$$\Phi^{c}_{\alpha} = \frac{t^c}{4} u^{d}_{3,\alpha} - \frac{1}{2} u^{d}_{3} u^{d}_{3,\alpha} - \frac{1}{2} u^{d}_{3} \overset{\circ}{u}{}^{d}_{3,\alpha} - \frac{1}{2} \overset{\circ}{u}{}^{d}_{3} u^{d}_{3,\alpha} - \Phi^{c}_{3} u^{c}_{3,\alpha} - \Phi^{c}_{3} \overset{\circ}{u}{}^{c}_{3,\alpha} + \frac{2}{5} \Phi^{c}_{3} \Phi^{c}_{3,\alpha} \tag{71}$$

$$\Omega^{c}_{\alpha} = -\frac{t^c}{6} \Phi_{3,\alpha} + \frac{2}{3} \Phi_{3} u^{d}_{3,\alpha} + \frac{2}{3} \Phi_{3} \overset{\circ}{u}{}^{d}_{3,\alpha} + \frac{1}{3} \Phi^{c}_{3,\alpha} u^{d}_{3} + \frac{1}{3} \Phi^{c}_{3,\alpha} \overset{\circ}{u}{}^{d}_{3}. \tag{72}$$

This result can be regarded as a specific simplifying kinematic assumption for the displacement functions Φ^{c}_{1}, Φ^{c}_{2}, Ω^{c}_{1} and Ω^{c}_{2}. Hence, the nonlinear 11-parameter shell theory defined by the kinematic equations (1)–(6) and (9)–(11), the equations of motion (41)–(49), the compatibility equation (62) and the corresponding boundary conditions (52)–(60) with the unknown displacement functions u^{a}_{i}, u^{d}_{i}, Φ^{c}_{i} and Ω^{c}_{α} can be reduced to a seven-parameter theory defined by the equations of motion (39)–(42) and (47)–(49) with the unknown displacement functions u^{a}_{i}, u^{d}_{i} and Φ^{c}_{3}. The reduction in the number of equations and unknown variables is caused by equilibrium requirements with respect to the stresses in the core of the sandwich panel which do not permit arbitrary displacements Φ^{c}_{α} and Ω^{c}_{α}. Eqs. (71) and (72) in the present form hold only for the case of orthotropic elasticity where the axes of orthotropy coincide with the axes x_i of the coordinate system and where the material behavior of the core is uniform with respect to the transverse direction x_3. Nevertheless, similar relations can be derived for other types of material behavior.

4. Analytical solution for simply supported sandwich panels

4.1. Transverse displacement functions

The sandwich shell theory derived in Sections 2 and 3 will be applied to buckling and postbuckling analyses of a simply supported rectangular sandwich panel with edge lengths l_1 and l_2 in the x_1- and x_2-directions, respectively. Along the panel edges, the transverse displacements u^{a}_{3} and u^{d}_{3} as well as the stress couples M^{a}_{nn} and M^{d}_{nn} are assumed to vanish. Furthermore, the tangential shear stress resultants N^{a}_{nt} and N^{d}_{nt} as well as the normal stress resultant N^{d}_{nn} along the edges vanish. With respect to normal stress resultants N^{a}_{nn} and the corresponding displacement function u^{a}_{n} two different cases are considered: For immovable edges, the displacement function u^{a}_{n} has to vanish whereas the stress resultant N^{a}_{nn} vanishes in the case of movable edges. The displacement function Φ^{c}_{3} is assumed to vanish throughout the area of the sandwich panel. Thus, no warping of the core in the transverse direction is considered while warping of the core is permitted with respect to the tangential directions.

A suitable representation for the transverse displacement functions in buckling and postbuckling problems is given by

$$u_3^{\mathrm{a}} = w_{mn}^{\mathrm{a}} \sin(\lambda_m^{\mathrm{a}} x_1) \sin(\mu_n^{\mathrm{a}} x_2), \quad \lambda_m^{\mathrm{a}} = \frac{m\pi}{l_1}, \quad \mu_n^{\mathrm{a}} = \frac{n\pi}{l_2} \tag{73}$$

$$u_3^{\mathrm{d}} = w_{pq}^{\mathrm{d}} \sin(\lambda_p^{\mathrm{d}} x_1) \sin(\mu_q^{\mathrm{d}} x_2), \quad \lambda_p^{\mathrm{d}} = \frac{p\pi}{l_1}, \quad \mu_q^{\mathrm{d}} = \frac{q\pi}{l_2} \tag{74}$$

where m, n, p and q are the number of sine half-waves in the corresponding directions whereas w_{mn}^{a} and w_{pq}^{d} denote the modal amplitudes of the corresponding transverse displacement function. The amplitudes remain unknown at this stage. The numbers of half-waves in the different parts of the solution are independent from each other.

For the initial geometric imperfection, a similar assumption

$$\overset{\circ}{u}_3^{\mathrm{a}} = \overset{\circ}{w}_{mn}^{\mathrm{a}} \sin(\lambda_m^{\mathrm{a}} x_1) \sin(\mu_n^{\mathrm{a}} x_2) \tag{75}$$

$$\overset{\circ}{u}_3^{\mathrm{d}} = \overset{\circ}{w}_{pq}^{\mathrm{d}} \sin(\lambda_p^{\mathrm{d}} x_1) \sin(\mu_q^{\mathrm{d}} x_2) \tag{76}$$

with the same numbers m, n, p and q is made. On the other hand, the amplitudes $\overset{\circ}{w}_{mn}^{\mathrm{a}}$ and $\overset{\circ}{w}_{pq}^{\mathrm{d}}$ of the initial geometric imperfection are independent from their load-dependent counterparts. As it was shown by Seide (1974), the initial geometric imperfection represented in a similar form as the buckling mode provides the most critical postbuckling conditions. Caused by the assumption of infinitesimal imperfections, the prescribed amplitudes of the imperfection have to be small compared to the overall dimensions of the sandwich panel under consideration.

4.2. Consistent solution for the tangential displacements

Similar to the procedure presented in the paper by Hause et al. (1998), a solution for the tangential displacement functions u_α^{a} and u_α^{d} can be derived, which is consistent with the assumptions (73)–(76) for the transverse displacements and the initial geometric imperfection.

Substituting the transverse displacement functions u_3^{a} and u_3^{d} as well as the initial geometric imperfections $\overset{\circ}{w}_{mn}^{\mathrm{a}}$ and $\overset{\circ}{w}_{pq}^{\mathrm{d}}$ according to Eqs. (73)–(76) into the compatibility condition (62) yields a partial differential equation for the average membrane strains $\bar{\gamma}_{\alpha\beta}^{\mathrm{a}}$ of the face sheets. Substituting the average membrane strain components in this equation with the inverted form of the material equations (63), and expressing the tangential stress resultants $N_{\alpha\beta}^{\mathrm{a}}$ in terms of the Airy stress function Φ using Eq. (61) results in an inhomogeneous partial differential equation for the Airy stress function.

The general solution of this differential equation reads

$$\begin{aligned}\Phi = {} & \frac{1}{2}\bar{N}_{11}^{\mathrm{a}}(x_2)^2 + \frac{1}{2}\bar{N}_{22}^{\mathrm{a}}(x_1)^2 + \left((w_{mn}^{\mathrm{a}})^2 + 2w_{mn}^{\mathrm{a}}\overset{\circ}{w}_{mn}^{\mathrm{a}}\right) C_1 \cos(2\lambda_m^{\mathrm{a}} x_1) + \left((w_{mn}^{\mathrm{a}})^2 + 2w_{mn}^{\mathrm{a}}\overset{\circ}{w}_{mn}^{\mathrm{a}}\right) C_2 \cos(2\mu_n^{\mathrm{a}} x_2) \\ & + w_{mn}^{\mathrm{a}} C_3 \sin(\lambda_m^{\mathrm{a}} x_1) \sin(\mu_n^{\mathrm{a}} x_2) + \left((w_{pq}^{\mathrm{d}})^2 + 2w_{pq}^{\mathrm{d}}\overset{\circ}{w}_{pq}^{\mathrm{d}}\right) C_4 \cos(2\lambda_p^{\mathrm{d}} x_1) + \left((w_{pq}^{\mathrm{d}})^2 + 2w_{pq}^{\mathrm{d}}\overset{\circ}{w}_{pq}^{\mathrm{d}}\right) C_5 \cos(2\mu_q^{\mathrm{d}} x_2)\end{aligned} \tag{77}$$

where $\bar{N}_{11}^{\mathrm{a}}$ and $\bar{N}_{22}^{\mathrm{a}}$ are the averages of the prescribed edge loads $\widehat{N}_{11}^{\mathrm{a}}$ and $\widehat{N}_{22}^{\mathrm{a}}$ at $x_1 = \text{constant}$ and $x_2 = \text{constant}$, respectively. The integration constants C_1–C_5 are obtained by substituting the general solution (77) into the differential equation and comparing the coefficients. Explicit expressions are given in Appendix B.

With the general solution (77) for the Airy stress function Φ, the average tangential stress resultants $N_{\alpha\beta}^{\mathrm{a}}$ are obtained from Eq. (61). These expressions are substituted into the first two relations of the constitutive equation (63). Replacing the average membrane strain components $\bar{\gamma}_{\alpha\beta}^{\mathrm{a}}$ with the explicit expressions given in Appendix A together with the representations (73)–(76) for the transverse displacements u_3^{a}, u_3^{d}, $\overset{\circ}{u}_3^{\mathrm{a}}$ and $\overset{\circ}{u}_3^{\mathrm{d}}$

yields a system of two coupled inhomogeneous partial differential equations for the average tangential face sheet displacements u_1^a and u_2^a. The system is solved by

$$\begin{aligned}
u_1^a = {} & \left((w_{mn}^a)^2 + 2w_{mn}^a \mathring{w}_{mn}^a\right) D_1 x_1 + \left((w_{mn}^a)^2 + 2w_{mn}^a \mathring{w}_{mn}^a\right) D_2 \sin(2\lambda_m^a x_1) \\
& + \left((w_{mn}^a)^2 + 2w_{mn}^a \mathring{w}_{mn}^a\right) D_3 \sin(2\lambda_m^a x_1)\cos(2\mu_n^a x_2) + \left((w_{pq}^d)^2 + 2w_{pq}^d \mathring{w}_{pq}^d\right) D_4 x_1 \\
& + \left((w_{pq}^d)^2 + 2w_{pq}^d \mathring{w}_{pq}^d\right) D_5 \sin(2\lambda_p^d x_1) + \left((w_{pq}^d)^2 + 2w_{pq}^d \mathring{w}_{pq}^d\right) D_6 \sin(2\lambda_p^d x_1)\cos(2\mu_q^d x_2) \\
& + w_{mn}^a D_7 \cos(\lambda_m^a x_1)\sin(\mu_n^a x_2) + D_8 \bar{N}_{11} x_1 + D_9 \bar{N}_{22} x_1
\end{aligned} \tag{78}$$

$$\begin{aligned}
u_2^a = {} & \left((w_{mn}^a)^2 + 2w_{mn}^a \mathring{w}_{mn}^a\right) E_1 x_2 + \left((w_{mn}^a)^2 + 2w_{mn}^a \mathring{w}_{mn}^a\right) E_2 \sin(2\mu_n^a x_2) \\
& + \left((w_{mn}^a)^2 + 2w_{mn}^a \mathring{w}_{mn}^a\right) E_3 \cos(2\lambda_m^a x_1)\sin(2\mu_n^a x_2) + \left((w_{pq}^d)^2 + 2w_{pq}^d \mathring{w}_{pq}^d\right) E_4 x_2 \\
& + \left((w_{pq}^d)^2 + 2w_{pq}^d \mathring{w}_{pq}^d\right) E_5 \sin(2\mu_q^d x_2) + \left((w_{pq}^d)^2 + 2w_{pq}^d \mathring{w}_{pq}^d\right) E_6 \cos(2\lambda_p^d x_1)\sin(2\mu_q^d x_2) \\
& + w_{mn}^a E_7 \sin(\lambda_m^a x_1)\cos(\mu_n^a x_2) + E_8 \bar{N}_{11} x_2 + E_9 \bar{N}_{22} x_2
\end{aligned} \tag{79}$$

where again the integration constants D_1–D_9 and E_1–E_9 are obtained by substituting the general solution (78) and (79) into the differential equations and comparing the coefficients. Explicit expressions for the integration constants are presented in Appendix B.

A consistent solution for the displacements u_1^d and u_2^d can be derived from the third and fourth equilibrium conditions (41) and (42). If the tangential stress resultants $N_{\alpha\beta}^d$ and the core stress resultants $N_{\alpha 3}^c$ in these relations are substituted by the respective constitutive equations in conjunction with the deformation components according to Appendix A, a system of two coupled inhomogeneous differential equations is obtained. The general solution of this system is given by

$$\begin{aligned}
u_1^d = {} & w_{mn}^a A_1 \cos(\lambda_m^a x_1)\sin(\mu_n^a x_2) + w_{pq}^d A_2 \cos(\lambda_p^d x_1)\sin(\mu_q^d x_2) \\
& + \left(w_{mn}^a w_{pq}^d + \mathring{w}_{mn}^a w_{pq}^d + w_{mn}^a \mathring{w}_{pq}^d\right) A_3 \cos(\lambda_m^a x_1)\sin(\mu_n^a x_2)\sin(\lambda_p^d x_1)\sin(\mu_q^d x_2) \\
& + \left(w_{mn}^a w_{pq}^d + \mathring{w}_{mn}^a w_{pq}^d + w_{mn}^a \mathring{w}_{pq}^d\right) A_4 \sin(\lambda_m^a x_1)\cos(\mu_n^a x_2)\cos(\lambda_p^d x_1)\cos(\mu_q^d x_2) \\
& + \left(w_{mn}^a w_{pq}^d + \mathring{w}_{mn}^a w_{pq}^d + w_{mn}^a \mathring{w}_{pq}^d\right) A_5 \sin(\lambda_m^a x_1)\sin(\mu_n^a x_2)\cos(\lambda_p^d x_1)\sin(\mu_q^d x_2) \\
& + \left(w_{mn}^a w_{pq}^d + \mathring{w}_{mn}^a w_{pq}^d + w_{mn}^a \mathring{w}_{pq}^d\right) A_6 \cos(\lambda_m^a x_1)\cos(\mu_n^a x_2)\sin(\lambda_p^d x_1)\cos(\mu_q^d x_2)
\end{aligned} \tag{80}$$

$$\begin{aligned}
u_2^d = {} & w_{mn}^a B_1 \sin(\lambda_m^a x_1)\cos(\mu_n^a x_2) + w_{pq}^d B_2 \sin(\lambda_p^d x_1)\cos(\mu_q^d x_2) \\
& + \left(w_{mn}^a w_{pq}^d + \mathring{w}_{mn}^a w_{pq}^d + w_{mn}^a \mathring{w}_{pq}^d\right) B_3 \sin(\lambda_m^a x_1)\cos(\mu_n^a x_2)\sin(\lambda_p^d x_1)\sin(\mu_q^d x_2) \\
& + \left(w_{mn}^a w_{pq}^d + \mathring{w}_{mn}^a w_{pq}^d + w_{mn}^a \mathring{w}_{pq}^d\right) B_4 \cos(\lambda_m^a x_1)\sin(\mu_n^a x_2)\cos(\lambda_p^d x_1)\cos(\mu_q^d x_2) \\
& + \left(w_{mn}^a w_{pq}^d + \mathring{w}_{mn}^a w_{pq}^d + w_{mn}^a \mathring{w}_{pq}^d\right) B_5 \sin(\lambda_m^a x_1)\sin(\mu_n^a x_2)\sin(\lambda_p^d x_1)\cos(\mu_q^d x_2) \\
& + \left(w_{mn}^a w_{pq}^d + \mathring{w}_{mn}^a w_{pq}^d + w_{mn}^a \mathring{w}_{pq}^d\right) B_6 \cos(\lambda_m^a x_1)\cos(\mu_n^a x_2)\cos(\lambda_p^d x_1)\sin(\mu_q^d x_2)
\end{aligned} \tag{81}$$

where the integration constants A_1 to A_6 and B_1 to B_6 are given in Appendix B.

With Eqs. (73)–(81), a consistent solution for the displacements u_i^{a} and u_i^{d} of the simply supported rectangular sandwich panels under consideration is obtained. The solution satisfies all boundary conditions of the simply supported panel with respect to the transverse displacements and with respect to the stress couples M_{nn}^{a} and M_{nn}^{d}. The boundary conditions with respect to the tangential displacements u_n^{d} and the tangential stress resultants N_{nn}^{a}, N_{nt}^{a}, N_{nn}^{d} and N_{nt}^{d} are satisfied in an integral average sense along the respective panel edges. Regarding the equations of motion, the first eight equations (39)–(46) are satisfied identically since they have been employed for the elimination of the tangential displacement functions Φ_α^{c} and $\Omega_\alpha^{\mathrm{c}}$ according to Eqs. (71) and (72) as well as for the determination of the consistent expressions (78)–(81) for the face sheet tangential displacements u_α^{a} and u_α^{d}. The only quantities in the solution (73)–(81) for the displacements u_i^{a} and u_i^{d} that remain unknown at this stage are the modal amplitudes w_{mn}^{a} and w_{pq}^{d} of the transverse displacements which have to be determined such that the last three equations of motion (47)–(49) are satisfied at least in an approximate sense.

4.3. Amplitudes of the transverse displacement functions

The unknown transverse displacement amplitudes are determined by means of an extended Galerkin scheme (Hause et al., 1998; Palazotto and Linnemann, 1991). Therefore, the solution (73)–(81) for the displacements of the panel together with the shell strain measures according to Appendix A and the constitutive equations (63)–(70) are substituted into the variational equation (28). Since the amplitudes of the transverse displacements are the only unknown quantities, the variations of the displacements and shell deformation components are expressed in terms of the variations $\delta w_{mn}^{\mathrm{a}}$ and $\delta w_{pq}^{\mathrm{d}}$ of the unknown modal amplitudes. Note that due to the vanishing transverse warping of the core the corresponding variation vanishes too ($\delta u_3^{\Phi} \equiv 0$). Hence, the eleventh equation of motion (49) becomes immaterial.

Neither the amplitudes of the transverse displacements nor their variations depend on the spatial position. Thus, the integral in Hamilton's principle can be evaluated. As the result, a single homogeneous equation is obtained, which depends linearly on the variations $\delta w_{mn}^{\mathrm{a}}$ and $\delta w_{pq}^{\mathrm{d}}$ of the unknown modal amplitudes. Since the variations of the transverse displacement amplitudes are arbitrary and independent, the corresponding coefficients must vanish independently. Thus, a system of two independent cubic equations for the two unknown displacement amplitudes w_{mn}^{a} and w_{pq}^{d} is obtained. In addition, this system depends on the prescribed average tangential edge loads $\bar{N}_{11}^{\mathrm{a}}$ and $\bar{N}_{22}^{\mathrm{a}}$, on the prescribed transverse normal loads $\hat{q}_3^{\mathrm{a}}$ and $\hat{q}_3^{\mathrm{d}}$ as well as on on the initial geometric imperfection amplitudes $\overset{\circ}{w}{}_{mn}^{\mathrm{a}}$ and $\overset{\circ}{w}{}_{pq}^{\mathrm{d}}$. Since the equations are rather lengthy, they are not presented in explicit form. The system is solved numerically by means of Newton's method.

5. Numerical examples

5.1. Flat panels under uniaxial in-plane compression

As a first example for the application of the methods derived in Sections 2–4, the buckling and post-buckling behavior of a flat sandwich panel under compressive uniaxial in-plane edge loads is considered. The panel under consideration has a square geometry with $l_1 = l_2 = 500$ mm and $r_1 = r_2 = \infty$. The face sheets are assumed to consist of aluminum with a Young's modulus of $E^{\mathrm{f}} = 70$ GPa, a Poisson's ratio of $\nu^{\mathrm{f}} = 0.3$ and a thickness of $t^{\mathrm{f}} = 1$ mm. The core material is also isotropic with transverse Young's and shear moduli of $E^{\mathrm{c}} = 0.7$ GPa and $G^{\mathrm{c}} = 0.269$ GPa, respectively, which is 1% of the corresponding moduli of the face sheets. Unless otherwise stated, a core thickness of $t^{\mathrm{c}} = 20$ mm is assumed. The sandwich panel is loaded in a pure uniaxial in-plane mode in the x_1-direction with $\bar{N}_{11}^{\mathrm{a}} \neq 0$ while the second average in-plane

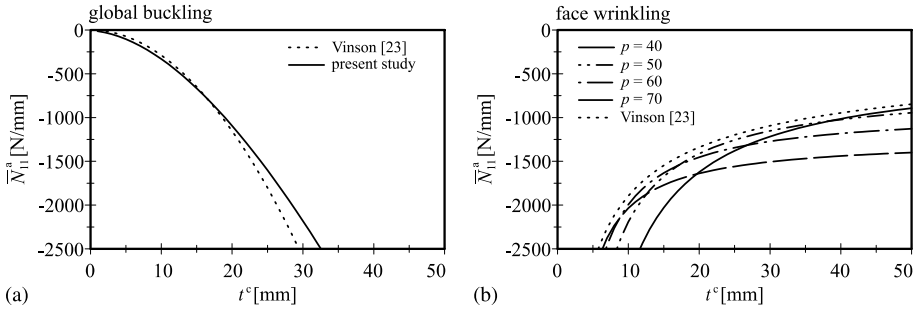

Fig. 2. Flat sandwich panel—buckling load.

stress resultant $\bar{N}_{22}^{a}$ vanishes. The edges parallel to the x_1-axis are movable within the x_1–x_2-plane. No transverse loads $\hat{q}_3^{a}$ and $\hat{q}_3^{d}$ are considered in the first example.

As a validation example, the buckling loads for the global instability as well as for the local, face wrinkling instability are determined as functions of the core thickness t^c. The results for both buckling modes are presented in Fig. 2. In this figure as well as in all subsequent figures, the standard sign convention is adopted that tensile loads are positive whereas compressive loads are negative. In order to obtain unperturbed results for a separated analysis of both cases, pure local and global buckling modes have been considered. Hence, in the analysis of the global buckling load, the amplitude w_{pq}^{d} of the face wrinkling instability is set to $w_{pq}^{d} \equiv 0$. Vice-versa, the amplitude w_{mn}^{a} is set to $w_{mn}^{a} \equiv 0$ in the analysis of the face wrinkling load. Needless to say, in the analysis of the buckling bifurcation loads no initial geometric imperfections are applied. For sake of comparison, the global and local buckling loads obtained by the approximate formulae given by Vinson (1999) are added as dotted lines. These approximate formulae are well verified by experimental results so that the numerical results obtained thereby can also be used for a validation of the present model.

Concerning the global buckling load, a progressive increase of the compressive load level $-\bar{N}_{11}^{a}$ with an increase in the core thickness t^c is observed. A rather good agreement between the results based on the present model and the ones by the approximate analysis using Vinson's (1999) formulae is observed for small to moderate core thicknesses t^c. A deviation develops for large core thicknesses. In this range, the approximation might be out of range of its validity. It should be noted that for a core thickness $t^c > 50$ mm, the ratio of the core thickness t^c to the in-plane dimension l_1 in the present example exceeds $1/10$ and thus might be out of the typical range for standard technological applications. The global buckling load is in all cases related to the buckling mode with $m = n = 1$ since this mode yields the lowest overall strain energy.

In contrast to the global buckling load, the face wrinkling load level $-\bar{N}_{11}^{a}$ decreases with increasing core thickness t^c. Furthermore, the buckling mode in this case depends on the core thickness. The number p of sine half-wave within the loading direction decreases with increasing core thickness due to the decreasing transverse normal stiffness of the core. On the other hand, a single sine half-wave $q = 1$ with respect to the x_2-direction normal to the external load $\bar{N}_{11}^{a}$ belongs to the lowest buckling mode. In all cases, the lowest compressive face wrinkling load for the respective core thickness is found to be in good agreement with the face wrinkling load obtained by Vinson's (1999) approximate formula. It should be noted that this approximate formula provides a clear bound on the compressive face wrinkling load levels obtained by the model used in the present study.

In Fig. 3, the load–deflection behavior in the postbuckling range of the flat sandwich panel is investigated. A constant core thickness of $t^c = 20$ mm is assumed. Again, pure buckling modes are considered where either the global deflection amplitude w_{mn}^{a} or the local deflection amplitude w_{pq}^{d} is considered to have a nonvanishing value. As in the previous investigation, the global buckling mode is given by $m = n = 1$ while a face wrinkling mode with $p = 53$ and $q = 1$ proves to correspond to the lowest buckling load for the face

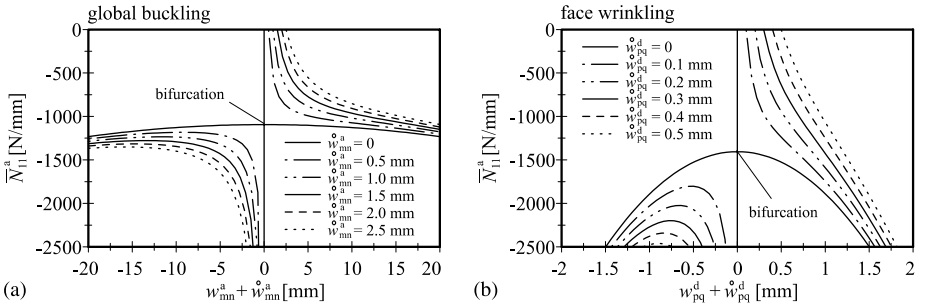

Fig. 3. Flat sandwich panel—postbuckling behavior.

wrinkling instability. In both cases, different values for the respective geometric imperfection are considered.

As it has to be expected, a buckling bifurcation is observed in both analyses only in the case of a geometrically perfect sandwich panel. The presence of an initial geometric imperfection results in a regularization of the load–deflection behavior so that no buckling in the Eulerian sense is present in these cases. It should be remarked that rather small initial geometric imperfections such as the wrinkling imperfection amplitude of $\overset{\circ}{w}{}^{\mathrm{d}}_{pq} = 0.1$ mm, have a significant effect on the load–deflection behavior especially in the vicinity of the respective bifurcation load level. If the bifurcation load is exceeded, a further increase in the load carrying capacity of the sandwich panel with both, an increasing amplitude w^{a}_{mn} of the global buckling mode, as well as an increasing amplitude w^{d}_{pq} of the face wrinkling mode is observed.

5.2. Cylindrical shell under axial compression

As a second example including curvature and interaction effects, the axial compression of a cylindrical sandwich shell with a rectangular projection on a plane is considered. The geometry is similar to that in the first example, except that a finite radius $r_2 = 2000$ mm within the x_2–x_3-plane is considered. Again the in-plane dimensions of the panel are $l_1 = l_2 = 500$ mm so that $r_2/l_2 = 4$ and $r_1/l_1 = \infty$. The core and face sheet thicknesses are $t^{\mathrm{c}} = 20$ mm and $t^{\mathrm{f}} = 1$ mm, respectively. The material properties of the core and face sheet material are given by $G^{\mathrm{c}} = 0.269$ GPa, $E^{\mathrm{c}} = 0.7$ GPa, $E^{\mathrm{f}} = 70$ GPa and $\nu^{\mathrm{f}} = 0.3$, respectively. The panel is loaded in a pure axial compression mode with $\bar{N}^{\mathrm{a}}_{11} \neq 0$ while all transverse distributed loads $\hat{q}^{\mathrm{a}}_3$ and $\hat{q}^{\mathrm{r}}_3$ are assumed to be zero. In contrast to the example regarding the flat sandwich panel, the edges parallel to the external loading direction (x_1-direction) are considered to be immovable with respect to the x_2-direction. Thus, a nonvanishing tangential stress resultant $\bar{N}^{\mathrm{a}}_{22}$ will in general be present in this example. In contrast to the previous analyses, in the remainder of this paper the global buckling mode and the face wrinkling instability will be considered in a coupled form.

In Fig. 4, the load–deflection behavior of the cylindrical shell is presented at different levels of the initial geometric imperfection amplitude $\overset{\circ}{w}{}^{\mathrm{a}}_{mn}$. A buckling mode with $m = n = q = 1$ and $p = 53$ is considered. This mode corresponds to the lowest strain energy level in the postbuckling range. In Fig. 4, the local imperfection amplitude $\overset{\circ}{w}{}^{\mathrm{d}}_{pq}$ is assumed to be zero. In contrast to the case of the flat sandwich panel, due to the panel curvature, a bifurcation in the global load–deflection diagram is obtained for a nonzero initial geometric imperfection with $\overset{\circ}{w}{}^{\mathrm{a}}_{mn} \approx 4.74$ mm. If for this geometric case the compressive load $-\bar{N}^{\mathrm{a}}_{11}$ is further increased, an unsymmetrical load–deflection behavior is observed. For slightly larger initial geometric imperfections than the value required for the occurrence of the bifurcation, a slight snap-through jump is observed due to the asymmetry of the load–deflection behavior in the postbuckling range. Again, strong effects of the initial geometric imperfection can be observed.

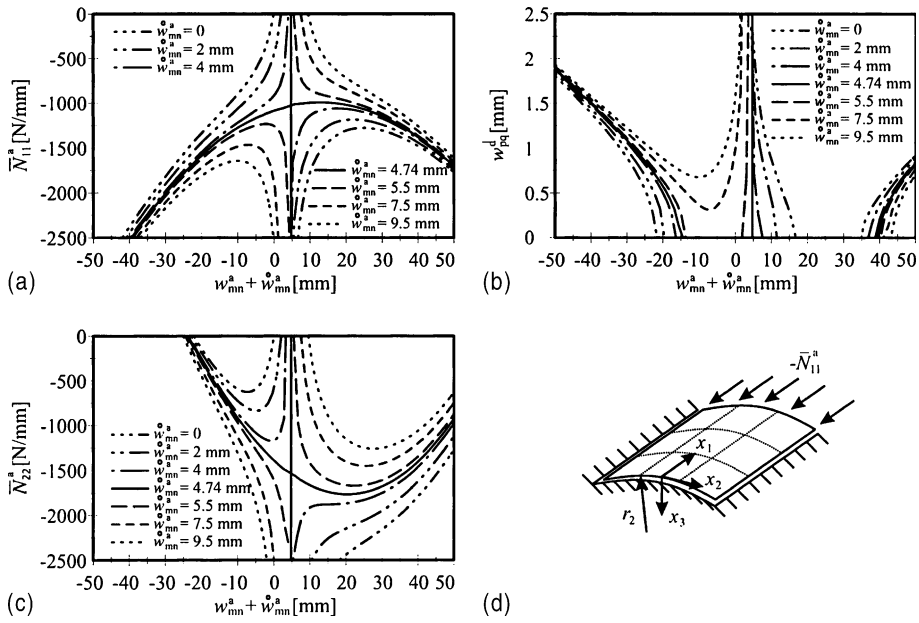

Fig. 4. Cylindrical sandwich panel—effect of global imperfection.

In the case of a global imperfection with $\overset{\circ}{w}{}^{a}_{mn} = 4.74$ mm, no face wrinkling instability is experienced, when the bifurcation load is reached. If the compressive load level is further increased, a second bifurcation occurs when the face wrinkling buckling load is reached. From this load level onwards, a nonvanishing local displacement $w^{d}_{pq} \neq 0$ is present (see Fig. 4b). The occurrence of this second bifurcation and the subsequent development of the local displacement w^{d}_{pq} essentially depends on the level of the global geometric imperfection $\overset{\circ}{w}{}^{a}_{mn}$. Since this imperfection has a strong effect on the global load–deflection behavior (see Fig. 4a), it strongly affects the overall load level $\bar{N}^{a}_{11}$ and thus also the occurrence and intensity of the local face wrinkling instability.

In Fig. 4c, the dependence of the induced stress resultant $\bar{N}^{a}_{22}$ normal to the loading (x_1-) direction is presented in dependence on the transverse deflection w^{a}_{mn}. For small compressive loads $\bar{N}^{a}_{11}$, which do not exceed the global buckling load, the stress resultant $\bar{N}^{a}_{22}$ normal to the loading direction is also negative due to the positive Poisson's ratios of the core and face sheet material. In the postbuckling range, a different behavior is observed. Due to the transverse deflection w^{a}_{mn}, an elongation of the panel with respect to x_2-direction occurs. At a sufficiently large load level, this elongation results in a sign change of the induced edge load $\bar{N}^{a}_{22}$. Especially for negative transverse deflections, this effect can be observed rather close to the bifurcation point.

In the previous analysis, a zero local imperfection $\overset{\circ}{w}{}^{d}_{pq}$ has been assumed. The effect of a nonvanishing local imperfection is investigated in Fig. 5. For a more comprehensive analysis of this effect, only the case of a unique global imperfection amplitude of $\overset{\circ}{w}{}^{a}_{mn} = 4.74$ mm is considered. This global imperfection corresponds to the only geometry, where a global bifurcation is obtained if no local imperfection is considered. In Fig. 5a, it can be observed that already small local geometric imperfections have a strong effect on the global load–deflection behavior. In agreement with the results presented by da Silva and Santos (1998), Sokolinsky and Frostig (2000) as well as by Wadee and Hunt (1998), this result outlines the fact that the global buckling mode and the local face wrinkling instability are strongly coupled effects due to nonlinear deformation coupling rather than being independent features.

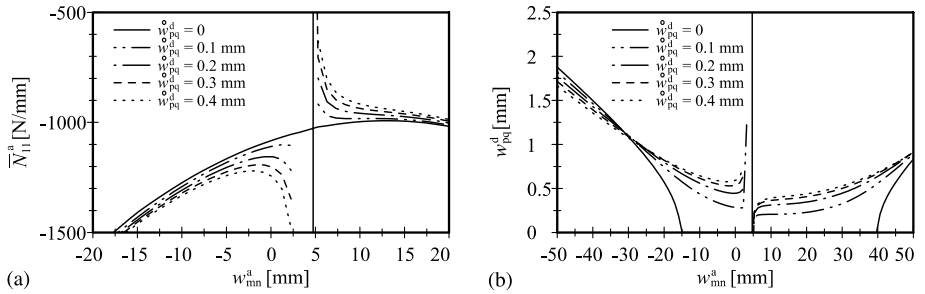

Fig. 5. Cylindrical sandwich panel—effect of local imperfection.

Strong effects of the local geometric imperfection are observed again with respect to the corresponding face wrinkling amplitude w^{d}_{pq} (see Fig. 5b). Although for zero initial geometric imperfections, no face wrinkling occurs for $w^{a}_{mn} \in [-15\text{ mm}, 39\text{ mm}]$, a significant, nonvanishing face wrinkling amplitude w^{d}_{pq} is observed in this interval, if a local geometric imperfection is present. Owing to a numerical instability of the employed solution procedure, no stable results were obtained in the vicinity of the the load–deflection curve without consideration of the local geometric imperfection.

In a final investigation concerning the cylindrical sandwich panel under axial compression, the effect of the radius of curvature r_2 on the deformation and buckling behavior is investigated. In Fig. 6a, the global load–deflection behavior is presented for four different radii of curvature. In Fig. 6b, the face wrinkling amplitude w^{d}_{pq} is presented as a function of the global transverse deflection w^{a}_{mn}. No local geometric imperfection is considered in the underlying analyses. The global imperfection amplitude for each radius of curvature is chosen in such a way that a global bifurcation is present. It can be observed that the global buckling load $-\bar{N}^{a}_{11}$ increases significantly with a decrease of the radius of curvature r_2. In addition, an increasing asymmetry of the load–deflection curve is observed. Thus, a more distinct snap-through jump develops for slightly larger imperfections than the considered ones. Due to the increased edge loads for small radii of curvature (i.e. for $r_2 = 500$ mm and $r_2 = 1000$ mm), a face wrinkling instability is experienced throughout the considered range of the global transverse deflection w^{a}_{mn}.

5.3. Spherical sandwich cap under unilateral transverse pressure

In the final example for application of the present model, the postbuckling behavior of a spherical sandwich cap with a square projection ($l_1 = l_2 = 500$ mm) and equal radii of curvature $r_1 = r_2 = r$ is investigated. Again, the panel has aluminum face sheets with $E^{f} = 70$ GPa, $\nu^{f} = 0.3$ and a thickness of $t^{f} = 1$ mm. The core material behavior is characterized by $G^{c} = 0.269$ GPa and $E^{c} = 0.7$ GPa. Unless otherwise

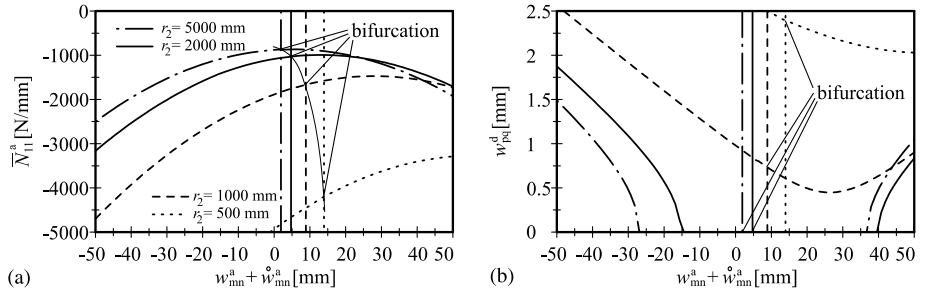

Fig. 6. Cylindrical sandwich panel—effect of radius of curvature.

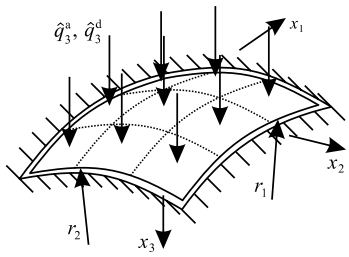

Fig. 7. Spherical sandwich cap—boundary and loading conditions.

specified, the core thickness is $t^c = 50$ mm and the radii of curvature are given by $r = 500$ mm. All edges of the sandwich cap are assumed to be immovable with respect to the direction normal to the respective edge. The sandwich cap is loaded by a constant unilateral transverse pressure with $\hat{q}_3^a = \hat{q}_3^d \neq 0$ (see Fig. 7). All subsequent results are related to a deformation mode with $m = n = q = 1$, and, depending on the considered geometry, an appropriate choice of p. No initial geometric imperfections are included throughout the remainder of this study.

In Fig. 8a, the load–deflection behavior for the spherical sandwich cap is presented for five different values of the core thickness t^c. In addition, the dependence of the face wrinkling amplitude w_{pq}^d (Fig. 8b) and the induced edge loads $\bar{N}_{11}^a$ and $\bar{N}_{22}^a$ (Fig. 8c and d) on the transverse deflection w_{mn}^a is investigated. For comparison, results are added where the face wrinkling instability is suppressed. These results are denoted by thin lines of the same type as the corresponding results in consideration of the face wrinkling instability mode.

With respect to the global load–deflection curve in the first plot in Fig. 8, no snap-trough effect is observed. Due to the high-bending stiffness of the sandwich cap under consideration, the global load–deflection behavior remains stable throughout the considered range. Nevertheless, the curvature characteristics of the load–deflection curves develop towards a snap-through effect if the core thickness t^c decreases. Since a

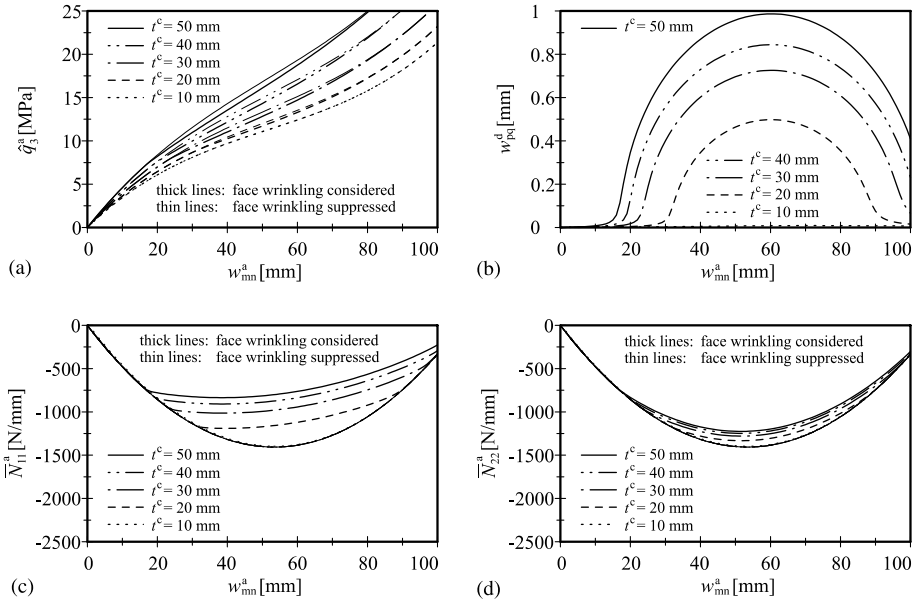

Fig. 8. Spherical sandwich cap—effect of core thickness.

positive transverse deflection w^{a}_{mn} of a spherical cap with immovable edges requires a shortening in the tangential dimensions, compressive average edge loads $-\bar{N}^{a}_{11}$ and $-\bar{N}^{a}_{22}$ develop as the transverse deflection is increased. If the curvature of the cap in the deformed configuration changes the sign at a sufficiently large transverse displacement w^{a}_{mn}, the increase in the level of the compressive edge loads is followed by a decrease and subsequently—at rather large deflections—by a change of sign into the tensile range.

If the level of the compressive edge loads $-\bar{N}^{a}_{11}$ and $-\bar{N}^{a}_{22}$ is sufficiently large, face wrinkling with a nonzero amplitude w^{d}_{pq} occurs. The only exception is the thin sandwich panel with $t^{c} = 10$ mm, where the face wrinkling load is not reached in the present example. Caused by the face wrinkling deformation, the face sheets become weaker, compared to the analysis, where the face wrinkling instability is suppressed. Therefore, a significant drop of the induced edge loads $-\bar{N}^{a}_{11}$ and $-\bar{N}^{a}_{22}$ is observed if face wrinkling is permitted. The drop is more significant with respect to $-\bar{N}^{a}_{11}$ since the buckling mode involving the lowest strain energy level is unsymmetrical. Note that the solution where the values of p and q are interchanged and thus the curves for $\bar{N}^{a}_{11}$ and $\bar{N}^{a}_{22}$ are also exchanged is equivalent to the present solution.

With respect to the global load $\hat{q}^{a}_{3}(=\hat{q}^{d}_{3})$, the effect caused by the occurrence of the face wrinkling instability is less distinct. Nevertheless, it should be noted that for core thickness of $t^{c} = 50$ mm and a fixed external load in the range 10 MPa $< \hat{q}^{a}_{3} <$ 15 MPa, the global deflection w^{a}_{mn} increases by $\approx$10%, if the face wrinkling instability is considered.

Finally, the effect of the radius of curvature r on the behavior of the previously analyzed sandwich cap with a core thickness of $t^{c} = 50$ mm is investigated. The results are presented in Fig. 9. A decrease of the radii of curvature r results in a decrease of the overall stiffness of the cap, and thus in a lower global load–deflection curve (see Fig. 9a). In addition, the deflection amplitudes w^{a}_{mn}, where the edge loads $\bar{N}^{a}_{11}$ and $\bar{N}^{a}_{22}$ become positive (implying tension), are shifted towards lower levels for large radii of curvature. In this case, the maximum compressive tangential stress level also decreases (see Fig. 9c and d). Since the face wrinkling bifurcation load is not exceeded for large radii of curvature, no face wrinkling occurs in these cases. Nevertheless, for moderate radii of curvature, minor effects are still present.

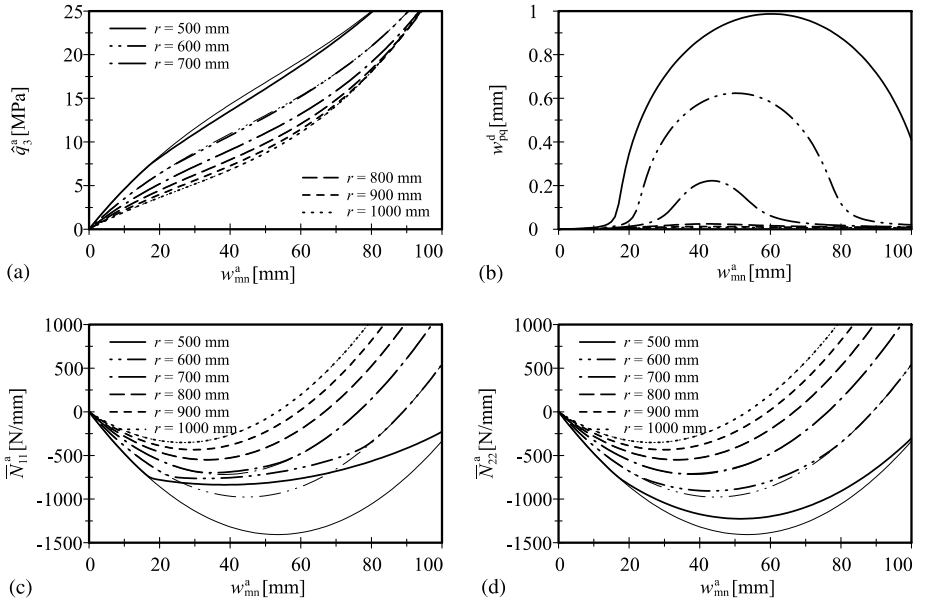

Fig. 9. Spherical sandwich cap—effect of radius of curvature.

6. Conclusions

The present study is concerned with the foundation of a comprehensive, geometrically nonlinear theory for doubly curved sandwich shells accounting for transverse core compressibility. Whereas the Kirchhoff–Love hypothesis is adopted for the face sheets, a $\{3,2\}$-order power series expansion is employed for the core displacements. The deformation of the shell is described in terms of the Green–Lagrange strain tensor in conjunction with the v. Kármán nonlinear model. Consistent equations of motion and the corresponding boundary conditions are derived by means of Hamilton's principle where inertia effects with respect to the transverse lateral degrees of freedom are included.

The distinguished feature of the present sandwich shell theory consists in its comprehensive formulation including all major effects such as transverse compressibility of the core, initial geometric imperfections, inertia effects, large transverse deflections and coupling effects induced by the panel curvature. Based on the postulated kinematic equations, all interaction effects are addressed in a natural manner. Especially with respect to the buckling and postbuckling behavior of sandwich panels, interactions of the global buckling mode and the local face wrinkling instability can be addressed. Since the model accounts for the transverse compressibility of the core, the face wrinkling instability is accessible during the structural analysis of the entire sandwich structure under consideration, rather than in a postanalysis based on approximate relations. Thus, all effects of the geometry and the global loading conditions on the face wrinkling instability can be analyzed directly. Furthermore, the effect of the face wrinkling instability on the global deformation and buckling behavior can be determined. In its basic form, the present sandwich shell theory is not restricted to any kind of specific constitutive relation for the core and face sheet material.

The derived shell theory is applied to static buckling and postbuckling analyses of simply supported rectangular sandwich panels. An analytical solution is derived for this problem in conjunction with orthotropic elasticity for both the core and the face sheets. The analytical solution is based on an assumed transverse displacement field in form of trigonometric functions. For the corresponding tangential displacements, a consistent solution is obtained by the subsequent solution of two systems of partial differential equations. The remaining unknowns are determined by means of an extended Galerkin procedure.

In three examples, the buckling and postbuckling behavior of flat and curved sandwich panels is investigated. Both, the overall buckling and the local face wrinkling instability modes are addressed. In addition, coupling effects are considered. Especially in the analysis of a spherical sandwich cap under transverse pressure, rather strong effects of the local face wrinkling mode on the induced tangential edge loads are observed. In addition, an initial geometric imperfection of the face wrinkling type is found to affect the global buckling behavior of a cylindrical sandwich panel under axial compression. These results reveal that the local face wrinkling instability is an important feature that intervenes with the global instability of structural sandwich panels. The refined theory of sandwich shells derived in the present study includes this effect, as well as all interactions of the local face sheet instability in a natural manner. The theory enables a refined, comprehensive high-precision analysis of structural sandwich panels accounting for all major effects. Finally, the remarkable computational efficiency of the analytical solution procedure employed in the present study should be emphasized.

Acknowledgements

The financial support of the Office of Naval Research, Composites Program, Grant N00014-02-1-0594, and the interest and encouragement of the Grant Monitor, Dr. Y.D.S. Rajapakse, are gratefully acknowledged.

Appendix A. Shell deformation components

The average and the half difference of the membrane strain components for the top and bottom face sheet are given by

$$\bar{\gamma}^{\mathrm{a}}_{11} = u^{\mathrm{a}}_{1,1} - \frac{1}{r_1}u^{\mathrm{a}}_3 + \frac{1}{2}(u^{\mathrm{a}}_{3,1})^2 + u^{\mathrm{a}}_{3,1}\overset{\circ}{u}{}^{\mathrm{a}}_{3,1} + \frac{1}{2}(u^{\mathrm{d}}_{3,1})^2 + u^{\mathrm{a}}_{3,1}\overset{\circ}{u}{}^{\mathrm{d}}_{3,1}$$

$$\bar{\gamma}^{\mathrm{a}}_{22} = u^{\mathrm{a}}_{2,2} - \frac{1}{r_2}u^{\mathrm{a}}_3 + \frac{1}{2}(u^{\mathrm{a}}_{3,2})^2 + u^{\mathrm{a}}_{3,1}\overset{\circ}{u}{}^{\mathrm{a}}_{3,2} + \frac{1}{2}(u^{\mathrm{d}}_{3,2})^2 + u^{\mathrm{a}}_{3,1}\overset{\circ}{u}{}^{\mathrm{d}}_{3,2}$$

$$\bar{\gamma}^{\mathrm{a}}_{12} = \frac{1}{2}u^{\mathrm{a}}_{1,2} + \frac{1}{2}u^{\mathrm{a}}_{2,1} + \frac{1}{2}u^{\mathrm{a}}_{3,1}u^{\mathrm{a}}_{3,2} + \frac{1}{2}u^{\mathrm{a}}_{3,1}\overset{\circ}{u}{}^{\mathrm{a}}_{3,2} + \frac{1}{2}\overset{\circ}{u}{}^{\mathrm{a}}_{3,1}u^{\mathrm{a}}_{3,2} + \frac{1}{2}u^{\mathrm{d}}_{3,1}u^{\mathrm{d}}_{3,2} + \frac{1}{2}u^{\mathrm{d}}_{3,1}\overset{\circ}{u}{}^{\mathrm{d}}_{3,2} + \frac{1}{2}\overset{\circ}{u}{}^{\mathrm{d}}_{3,1}u^{\mathrm{d}}_{3,2}$$

$$\bar{\gamma}^{\mathrm{d}}_{11} = u^{\mathrm{d}}_{1,1} - \frac{1}{r_1}u^{\mathrm{d}}_3 + u^{\mathrm{a}}_{3,1}u^{\mathrm{d}}_{3,1} + u^{\mathrm{a}}_{3,1}\overset{\circ}{u}{}^{\mathrm{d}}_{3,1} + \overset{\circ}{u}{}^{\mathrm{a}}_{3,1}u^{\mathrm{d}}_{3,1}$$

$$\bar{\gamma}^{\mathrm{d}}_{22} = u^{\mathrm{d}}_{2,2} - \frac{1}{r_2}u^{\mathrm{d}}_3 + u^{\mathrm{a}}_{3,2}u^{\mathrm{d}}_{3,2} + u^{\mathrm{a}}_{3,2}\overset{\circ}{u}{}^{\mathrm{d}}_{3,2} + \overset{\circ}{u}{}^{\mathrm{a}}_{3,2}u^{\mathrm{d}}_{3,2}$$

$$\bar{\gamma}^{\mathrm{d}}_{11} = \frac{1}{2}u^{\mathrm{d}}_{1,2} + \frac{1}{2}u^{\mathrm{d}}_{2,1} + \frac{1}{2}u^{\mathrm{a}}_{3,1}u^{\mathrm{d}}_{3,2} + \frac{1}{2}u^{\mathrm{a}}_{3,1}\overset{\circ}{u}{}^{\mathrm{d}}_{3,2} + \frac{1}{2}\overset{\circ}{u}{}^{\mathrm{a}}_{3,1}u^{\mathrm{d}}_{3,2} + \frac{1}{2}u^{\mathrm{a}}_{3,2}u^{\mathrm{d}}_{3,1} + \frac{1}{2}u^{\mathrm{a}}_{3,2}\overset{\circ}{u}{}^{\mathrm{d}}_{3,1} + \frac{1}{2}\overset{\circ}{u}{}^{\mathrm{a}}_{3,2}u^{\mathrm{d}}_{3,1}.$$

The bending strains for the face sheets read

$$\kappa^{\mathrm{a}}_{11} = -u^{\mathrm{a}}_{3,11}$$

$$\kappa^{\mathrm{a}}_{22} = -u^{\mathrm{a}}_{3,22}$$

$$\kappa^{\mathrm{a}}_{12} = -u^{\mathrm{a}}_{3,12}$$

$$\kappa^{\mathrm{d}}_{11} = -u^{\mathrm{d}}_{3,11}$$

$$\kappa^{\mathrm{d}}_{22} = -u^{\mathrm{d}}_{3,22}$$

$$\kappa^{\mathrm{d}}_{12} = -u^{\mathrm{d}}_{3,12}.$$

The deformation components of the core layer are given by

$$\bar{\gamma}^{\mathrm{c}}_{33} = -\frac{2}{t^{\mathrm{c}}}u^{\mathrm{d}}_3 + \frac{2}{(t^{\mathrm{c}})^2}(u^{\mathrm{d}}_3)^2 + \frac{4}{(t^{\mathrm{c}})^2}u^{\mathrm{d}}_3\overset{\circ}{u}{}^{\mathrm{d}}_3 + \frac{8}{(t^{\mathrm{c}})^2}(\Phi^{\mathrm{c}}_3)^2$$

$$\bar{\gamma}^{\mathrm{c}}_{23} = -\frac{1}{t^{\mathrm{c}}}u^{\mathrm{d}}_2 + \frac{t^{\mathrm{c}}+t^{\mathrm{f}}}{2t^{\mathrm{c}}}u^{\mathrm{a}}_{3,2} + \frac{2}{t^{\mathrm{c}}}\Omega^{\mathrm{c}}_2 - \frac{1}{t^{\mathrm{c}}}u^{\mathrm{a}}_{3,2}u^{\mathrm{d}}_3 - \frac{1}{t^{\mathrm{c}}}u^{\mathrm{a}}_{3,2}\overset{\circ}{u}{}^{\mathrm{d}}_3 - \frac{1}{t^{\mathrm{c}}}\overset{\circ}{u}{}^{\mathrm{a}}_{3,2}u^{\mathrm{d}}_3 - \frac{2}{t^{\mathrm{c}}}u^{\mathrm{d}}_{3,2}\Phi^{\mathrm{c}}_3 - \frac{2}{t^{\mathrm{c}}}\overset{\circ}{u}{}^{\mathrm{d}}_{3,2}\Phi^{\mathrm{c}}_3$$

$$\bar{\gamma}^{\mathrm{c}}_{13} = -\frac{1}{t^{\mathrm{c}}}u^{\mathrm{d}}_1 + \frac{t^{\mathrm{c}}+t^{\mathrm{f}}}{2t^{\mathrm{c}}}u^{\mathrm{a}}_{3,1} + \frac{2}{t^{\mathrm{c}}}\Omega^{\mathrm{c}}_1 - \frac{1}{t^{\mathrm{c}}}u^{\mathrm{a}}_{3,1}u^{\mathrm{d}}_3 - \frac{1}{t^{\mathrm{c}}}u^{\mathrm{a}}_{3,1}\overset{\circ}{u}{}^{\mathrm{d}}_3 - \frac{1}{t^{\mathrm{c}}}\overset{\circ}{u}{}^{\mathrm{a}}_{3,1}u^{\mathrm{d}}_3 - \frac{2}{t^{\mathrm{c}}}u^{\mathrm{d}}_{3,1}\Phi^{\mathrm{c}}_3 - \frac{2}{t^{\mathrm{c}}}\overset{\circ}{u}{}^{\mathrm{d}}_{3,1}\Phi^{\mathrm{c}}_3$$

$$\kappa^{\mathrm{c}}_{33} = \frac{8}{(t^{\mathrm{c}})^2} - \frac{16}{(t^{\mathrm{c}})^3}u^{\mathrm{d}}_3\Phi^{\mathrm{c}}_3 - \frac{16}{(t^{\mathrm{c}})^3}\overset{\circ}{u}{}^{\mathrm{d}}_3\Phi^{\mathrm{c}}_3$$

$$\kappa^{\mathrm{c}}_{23} = -\frac{1}{t^{\mathrm{c}}}u^{\mathrm{d}}_{3,2} + \frac{4}{(t^{\mathrm{c}})^2}\Phi^{\mathrm{c}}_2 + \frac{2}{(t^{\mathrm{c}})^2}u^{\mathrm{d}}_3u^{\mathrm{d}}_{3,2} + \frac{2}{(t^{\mathrm{c}})^2}u^{\mathrm{d}}_3\overset{\circ}{u}{}^{\mathrm{d}}_{3,2} + \frac{2}{(t^{\mathrm{c}})^2}\overset{\circ}{u}{}^{\mathrm{d}}_3u^{\mathrm{d}}_{3,2} + \frac{4}{(t^{\mathrm{c}})^2}u^{\mathrm{a}}_{3,2}\Phi^{\mathrm{c}}_3 + \frac{4}{(t^{\mathrm{c}})^2}\overset{\circ}{u}{}^{\mathrm{a}}_{3,2}\Phi^{\mathrm{c}}_3$$

$$\kappa^{\mathrm{c}}_{13} = -\frac{1}{t^{\mathrm{c}}}u^{\mathrm{d}}_{3,1} + \frac{4}{(t^{\mathrm{c}})^2}\Phi^{\mathrm{c}}_1 + \frac{2}{(t^{\mathrm{c}})^2}u^{\mathrm{d}}_3u^{\mathrm{d}}_{3,1} + \frac{2}{(t^{\mathrm{c}})^2}u^{\mathrm{d}}_3\overset{\circ}{u}{}^{\mathrm{d}}_{3,1} + \frac{2}{(t^{\mathrm{c}})^2}\overset{\circ}{u}{}^{\mathrm{d}}_3u^{\mathrm{d}}_{3,1} + \frac{4}{(t^{\mathrm{c}})^2}u^{\mathrm{a}}_{3,1}\Phi^{\mathrm{c}}_3 + \frac{4}{(t^{\mathrm{c}})^2}\overset{\circ}{u}{}^{\mathrm{a}}_{3,1}\Phi^{\mathrm{c}}_3$$

$$\eta^{\mathrm{c}}_{33} = \frac{32}{(t^{\mathrm{c}})^4}(\Phi^{\mathrm{c}}_3)^2$$

$$\eta^{\mathrm{c}}_{23} = \frac{2}{(t^{\mathrm{c}})^2}\Phi^{\mathrm{c}}_{3,2} + \frac{12}{(t^{\mathrm{c}})^3}\Omega^{\mathrm{c}}_2 - \frac{8}{(t^{\mathrm{c}})^3}u^{\mathrm{d}}_{3,2}\Phi^{\mathrm{c}}_3 - \frac{8}{(t^{\mathrm{c}})^3}\overset{\circ}{u}{}^{\mathrm{d}}_{3,2}\Phi^{\mathrm{c}}_3 - \frac{4}{(t^{\mathrm{c}})^3}u^{\mathrm{d}}_3\Phi^{\mathrm{c}}_{3,2} - \frac{4}{(t^{\mathrm{c}})^3}\overset{\circ}{u}{}^{\mathrm{d}}_3\Phi^{\mathrm{c}}_{3,2}$$

$$\eta_{13}^{c} = \frac{2}{(t^c)^2}\Phi_{3,1}^{c} + \frac{12}{(t^c)^3}\Omega_1^{c} - \frac{8}{(t^c)^3}u_{3,1}^{d}\Phi_3^{c} - \frac{8}{(t^c)^3}\overset{\circ}{u}{}_{3,1}^{d}\Phi_3^{c} - \frac{4}{(t^c)^3}u_3^{d}\Phi_{3,1}^{c} - \frac{4}{(t^c)^3}\overset{\circ}{u}{}_3^{d}\Phi_{3,1}^{c}$$

$$\vartheta_{33}^{c} = 0$$

$$\vartheta_{23}^{c} = \frac{16}{(t^c)^4}\Phi_3^{c}\Phi_{3,2}^{c}$$

$$\vartheta_{13}^{c} = \frac{16}{(t^c)^4}\Phi_3^{c}\Phi_{3,1}^{c}.$$

Appendix B. Integration constants

The integration constants in the general solution (77) for the Airy stress function are given by

$$C_1 = \frac{1}{32}\frac{(\mu_n^a)^2}{(\lambda_m^a)^2}\frac{A_{11}^f A_{22}^f - (A_{12}^f)^2}{A_{11}^f}$$

$$C_2 = \frac{1}{32}\frac{(\lambda_m^a)^2}{(\mu_n^a)^2}\frac{A_{11}^f A_{22}^f - (A_{12}^f)^2}{A_{22}^f}$$

$$C_3 = \frac{\left(\frac{(\mu_n^a)^2}{r_1} + \frac{(\lambda_n^a)^2}{r_2}\right)\left(A_{11}^f A_{22}^f A_{66}^f - (A_{12}^f)^2 A_{66}^f\right)}{(\lambda_m^a)^4 A_{11}^f A_{66}^f + (\lambda_m^a)^2(\mu_n^a)^2\left(A_{11}^f A_{22}^f - (A_{12}^f)^2 - 2A_{12}^f A_{66}^f\right) + (\mu_n^a)^4 A_{22}^f A_{66}^f}$$

$$C_4 = \frac{1}{32}\frac{(\mu_q^d)^2}{(\lambda_p^d)^2}\frac{A_{11}^f A_{22}^f - (A_{12}^f)^2}{A_{11}^f}$$

$$C_5 = \frac{1}{32}\frac{(\lambda_p^d)^2}{(\mu_q^d)^2}\frac{A_{11}^f A_{22}^f - (A_{12}^f)^2}{A_{22}^f}.$$

The integration constants in the solution (78) and (79) for the average tangential displacements are given by

$$D_1 = -\frac{1}{8}(\lambda_m^a)^2$$

$$D_2 = \frac{1}{16}\frac{(\mu_n^a)^2 A_{12}^f - (\lambda_m^a)^2 A_{11}^a}{\lambda_m^a A_{11}^f}$$

$$D_3 = \frac{1}{16}\lambda_m^a$$

$$D_4 = -\frac{1}{\lambda_m^a r_1} + \frac{(\mu_n^a)^2 A_{22}^f - (\lambda_m^a)^2 A_{12}^f}{\lambda_m^a\left(A_{11}^f A_{22}^f - (A_{12}^f)^2\right)}C_3$$

$$D_5 = \frac{A_{22}^f}{A_{11}^f A_{22}^f - (A_{12}^f)^2}$$

$$D_6 = -\frac{A_{12}^f}{A_{11}^f A_{22}^f - (A_{12}^f)^2}$$

$$D_7 = -\frac{1}{8}(\lambda_p^d)^2$$

$$D_8 = \frac{1}{16}\frac{(\mu_q^{\mathrm{d}})^2 A_{12}^{\mathrm{f}} - (\lambda_p^{\mathrm{d}})^2 A_{11}^{\mathrm{a}}}{\lambda_p^{\mathrm{d}} A_{11}^{\mathrm{f}}}$$

$$D_9 = \frac{1}{16}\lambda_p^{\mathrm{d}}$$

$$E_1 = -\frac{1}{8}(\mu n^{\mathrm{a}})^2$$

$$E_2 = \frac{1}{16}\frac{(\lambda_m^{\mathrm{a}})^2 A_{12}^{\mathrm{f}} - (\mu_n^{\mathrm{a}})^2 A_{22}^{\mathrm{a}}}{\mu_n^{\mathrm{a}} A_{22}^{\mathrm{f}}}$$

$$E_3 = \frac{1}{16}\mu_n^{\mathrm{a}}$$

$$E_4 = -\frac{1}{\mu_n^{\mathrm{a}} r_2} + \frac{(\lambda_m^{\mathrm{a}})^2 A_{11}^{\mathrm{f}} - (\mu_n^{\mathrm{a}})^2 A_{12}^{\mathrm{f}}}{\mu_n^{\mathrm{a}}\left(A_{11}^{\mathrm{f}} A_{22}^{\mathrm{f}} - (A_{12}^{\mathrm{f}})^2\right)} C_3$$

$$E_5 = -\frac{A_{12}^{\mathrm{f}}}{A_{11}^{\mathrm{f}} A_{22}^{\mathrm{f}} - (A_{12}^{\mathrm{f}})^2}$$

$$E_6 = \frac{A_{11}^{\mathrm{f}}}{A_{11}^{\mathrm{f}} A_{22}^{\mathrm{f}} - (A_{12}^{\mathrm{f}})^2}$$

$$E_7 = -\frac{1}{8}(\mu_q^{\mathrm{d}})^2$$

$$E_8 = \frac{1}{16}\frac{(\lambda_p^{\mathrm{d}})^2 A_{12}^{\mathrm{f}} - (\mu_q^{\mathrm{d}})^2 A_{22}^{\mathrm{a}}}{\mu_q^{\mathrm{d}} A_{22}^{\mathrm{f}}}$$

$$E_9 = \frac{1}{16}\mu_q^{\mathrm{d}}.$$

The integration constants in the expressions (80) and (81) for the half difference of the face sheet tangential displacements are obtained as the solution of the following linear systems:

$$\begin{pmatrix} M_1 & M_2 \\ (\mathrm{Sym.}) & M_3 \end{pmatrix}\begin{pmatrix} A_1 \\ B_1 \end{pmatrix} = \begin{pmatrix} R_1 \\ R_2 \end{pmatrix}$$

with

$$M_1 = (\lambda_m^{\mathrm{a}})^2 A_{11}^{\mathrm{f}} + (\mu_n^{\mathrm{a}})^2 A_{66}^{\mathrm{f}} + \frac{2}{(t^{\mathrm{c}})^2} A_{55}^{\mathrm{c}}$$

$$M_2 = \lambda_m^{\mathrm{a}}\mu_n^{\mathrm{a}}\left(A_{12}^{\mathrm{f}} + A_{66}^{\mathrm{f}}\right)$$

$$M_3 = (\mu_n^{\mathrm{a}})^2 A_{22}^{\mathrm{f}} + (\lambda_m^{\mathrm{a}})^2 A_{66}^{\mathrm{f}} + \frac{2}{(t^{\mathrm{c}})^2} A_{44}^{\mathrm{c}}$$

$$R_1 = \lambda_m^{\mathrm{a}}\frac{t^{\mathrm{c}} + t^{\mathrm{f}}}{(t^{\mathrm{c}})^2} A_{55}^{\mathrm{c}}$$

$$R_2 = \mu_n^{\mathrm{a}}\frac{t^{\mathrm{c}} + t^{\mathrm{f}}}{(t^{\mathrm{c}})^2} A_{44}^{\mathrm{c}},$$

$$\begin{pmatrix} M_4 & M_5 \\ (\mathrm{Sym.}) & M_6 \end{pmatrix}\begin{pmatrix} A_2 \\ B_2 \end{pmatrix} = \begin{pmatrix} R_3 \\ R_4 \end{pmatrix}$$

with

$$M_4 = (\lambda_p^{\mathrm{d}})^2 A_{11}^{\mathrm{f}} + (\mu_q^{\mathrm{d}})^2 A_{66}^{\mathrm{f}} + \frac{2}{(t^{\mathrm{c}})^2} A_{55}^{\mathrm{c}}$$

$$M_5 = \lambda_p^{\mathrm{d}} \mu_q^{\mathrm{d}} \left(A_{12}^{\mathrm{f}} + A_{66}^{\mathrm{f}}\right)$$

$$M_6 = (\mu_q^{\mathrm{d}})^2 A_{22}^{\mathrm{f}} + (\lambda_p^{\mathrm{d}})^2 A_{66}^{\mathrm{f}} + \frac{2}{(t^{\mathrm{c}})^2} A_{44}^{\mathrm{c}}$$

$$R_3 = -\lambda_p^{\mathrm{d}} \left(\frac{1}{r_1} A_{11}^{\mathrm{f}} + \frac{1}{r_2} A_{12}^{\mathrm{f}} \right)$$

$$R_4 = -\mu_q^{\mathrm{d}} \left(\frac{1}{r_1} A_{12}^{\mathrm{f}} + \frac{1}{r_2} A_{22}^{\mathrm{f}} \right)$$

$$\begin{pmatrix} M_7 & 0 & M_9 & -M_{11} & M_{13} & -M_{14} & M_{15} & M_{16} \\ & M_7 & -M_{11} & M_9 & -M_{14} & M_{13} & -M_{16} & M_{15} \\ & & M_7 & 0 & M_{16} & -M_{15} & M_{14} & -M_{13} \\ & & & M_7 & -M_{15} & M_{16} & -M_{13} & M_{14} \\ & & & & M_8 & 0 & M_{10} & -M_{12} \\ & & & & & M_8 & -M_{12} & M_{10} \\ & \text{(Sym.)} & & & & & M_8 & 0 \\ & & & & & & & M_8 \end{pmatrix} \begin{pmatrix} A_3 \\ A_4 \\ A_5 \\ A_6 \\ B_3 \\ B_4 \\ B_5 \\ B_6 \end{pmatrix} = \begin{pmatrix} R_5 \\ R_6 \\ R_7 \\ R_8 \\ R_9 \\ R_{10} \\ R_{11} \\ R_{12} \end{pmatrix}$$

with

$$M_7 = \left((\lambda_m^{\mathrm{a}})^2 + (\lambda_p^{\mathrm{d}})^2\right) A_{11}^{\mathrm{f}} + \left((\mu_n^{\mathrm{a}})^2 + (\mu_q^{\mathrm{d}})^2\right) A_{66}^{\mathrm{f}} + \frac{2}{(t^{\mathrm{c}})^2} A_{55}^{\mathrm{c}}$$

$$M_8 = \left((\mu_n^{\mathrm{a}})^2 + (\mu_q^{\mathrm{d}})^2\right) A_{22}^{\mathrm{f}} + \left((\lambda_m^{\mathrm{a}})^2 + (\lambda_p^{\mathrm{d}})^2\right) A_{66}^{\mathrm{f}} + \frac{2}{(t^{\mathrm{c}})^2} A_{44}^{\mathrm{c}}$$

$$M_9 = 2\lambda_m^{\mathrm{a}} \lambda_p^{\mathrm{d}} A_{11}^{\mathrm{f}}$$

$$M_{10} = 2\mu_n^{\mathrm{a}} \mu_q^{\mathrm{d}} A_{22}^{\mathrm{f}}$$

$$M_{11} = 2\mu_n^{\mathrm{a}} \mu_q^{\mathrm{d}} A_{66}^{\mathrm{f}}$$

$$M_{12} = 2\lambda_m^{\mathrm{a}} \lambda_p^{\mathrm{d}} A_{66}^{\mathrm{f}}$$

$$M_{13} = \lambda_m^{\mathrm{a}} \mu_n^{\mathrm{a}} \left(A_{12}^{\mathrm{f}} + A_{66}^{\mathrm{f}}\right)$$

$$M_{14} = \lambda_p^{\mathrm{d}} \mu_q^{\mathrm{d}} \left(A_{12}^{\mathrm{f}} + A_{66}^{\mathrm{f}}\right)$$

$$M_{15} = \lambda_m^{\mathrm{a}} \mu_q^{\mathrm{d}} \left(A_{12}^{\mathrm{f}} + A_{66}^{\mathrm{f}}\right)$$

$$M_{16} = \lambda_p^{\mathrm{d}} \mu_n^{\mathrm{a}} \left(A_{12}^{\mathrm{f}} + A_{66}^{\mathrm{f}}\right)$$

$$R_5 = -\lambda_m^{\mathrm{a}} \left((\lambda_p^{\mathrm{d}})^2 A_{11}^{\mathrm{f}} + (\mu_q^{\mathrm{d}})^2 A_{66}^{\mathrm{f}} + \frac{2}{(t^{\mathrm{c}})^2} A_{55}^{\mathrm{c}} \right)$$

$$R_6 = \mu_n^{\mathrm{a}} \lambda_p^{\mathrm{d}} \mu_q^{\mathrm{d}} \left(A_{12}^{\mathrm{f}} + A_{66}^{\mathrm{f}}\right)$$

$$R_7 = -\lambda_p^{\mathrm{d}} \left((\lambda_m^{\mathrm{a}})^2 A_{11}^{\mathrm{f}} + (\mu_n^{\mathrm{a}})^2 A_{66}^{\mathrm{f}} \right)$$

$$R_8 = \mu_q^{\mathrm{d}} \lambda_m^{\mathrm{a}} \mu_n^{\mathrm{a}} \left(A_{12}^{\mathrm{f}} + A_{66}^{\mathrm{f}}\right)$$

$$R_9 = -\mu_n^{\mathrm{a}}\left((\mu_q^{\mathrm{d}})^2 A_{22}^{\mathrm{f}} + (\lambda_p^{\mathrm{d}})^2 A_{66}^{\mathrm{f}} + \frac{2}{(t^{\mathrm{c}})^2} A_{44}^{\mathrm{c}}\right)$$

$$R_{10} = \lambda_m^{\mathrm{a}}\lambda_p^{\mathrm{d}}\mu_q^{\mathrm{d}}\left(A_{12}^{\mathrm{f}} + A_{66}^{\mathrm{f}}\right)$$

$$R_{11} = -\mu_q^{\mathrm{d}}\left((\mu_n^{\mathrm{a}})^2 A_{22}^{\mathrm{f}} + (\lambda_m^{\mathrm{a}})^2 A_{66}^{\mathrm{f}}\right)$$

$$R_{12} = \lambda_p^{\mathrm{d}}\lambda_m^{\mathrm{a}}\mu_n^{\mathrm{a}}\left(A_{12}^{\mathrm{f}} + A_{66}^{\mathrm{f}}\right).$$

Since the results are rather lengthy, the solutions are not presented in explicit form.

References

Allen, H.G., 1969. Analysis and Design of Structural Sandwich Panels. Pergamon Press, Oxford.

Barut, A., Madenci, E., Heinrich, J., Tessler, A., 2001. Analysis of thick sandwich construction by a {3, 2}-order theory. International Journal of Solids and Structures 38, 6063–6077.

Bozhevolnaya, E., Frostig, Y., 1997. Nonlinear closed-form high-order analysis of curved sandwich panels. Composite Structures 38, 383–394.

da Silva, L.A.P.S., Santos, J.M.C., 1998. Localised formulations for thick "sandwich" laminated and composite structures. Computational Mechanics 22, 211–224.

Dawe, D.J., Yuan, W.X., 2001. Overall and local buckling of sandwich plates with laminated faceplates. Part I: analysis. Computer Methods in Applied Mechanics and Engineering 190, 5197–5213.

Ferreira, J.M., Barbosa, J.T., Torres Marques, A., César de Sá, J., 2000. Non-linear analysis of sandwich shells: the effect of core plasticity. Computers and Structures 76, 337–346.

Frostig, Y., 1998. Buckling of sandwich panels with a flexible core—high-order theory. International Journal of Solids and Structures 35, 183–204.

Frostig, Y., Baruch, M., Vilnay, O., Sheiman, I., 1992. High-order buckling theory for sandwich-beam behavior with transversely flexible core. Journal of Engineering Mechanics 118, 1026–1043.

Hao, B., Cho, C., Lee, S.W., 2000. Buckling and postbuckling of soft-core sandwich plates with composite facesheets. Computational Mechanics 25, 421–429.

Hause, T., Librescu, L., Camarda, C.J., 1998. Postbuckling of anisotropic flat and doubly-curved sandwich panels under complex loading conditions. International Journal of Solids and Structures 35, 3007–3027.

Lewiński, T., 1991. On displacement-based theories of sandwich plates with soft core. Journal of Engineering Mathematics 25, 223–241.

Librescu, L., Chang, M.Y., 1993. Effects of geometric imperfections on vibration of compressed shear deformable composite curved panels. Acta Mechanica 96, 203–224.

Librescu, L., Hause, T., 2000. Recent developments in the modeling and behavior of advanced sandwich constructions: a survey. Composite Structures 48, 1–17.

Librescu, L., Hause, C., Camarda, C.J., 1997. Geometrically nonlinear theory of initially imperfect sandwich curved panels incorporating nonclassical effects. AIAA Journal 35, 1393–1403.

Mouritz, A.P., Gellert, E., Burchhill, P., Challis, K., 2001. Review of advanced composite structures for naval ships and submarines. Composite Structures 53, 21–41.

Noor, A.K., Burton, W.S., Bert, C.W., 1996. Computational models for sandwich panels and shells. Applied Mechanics Reviews 49, 155–199.

Pai, P.F., Palazotto, A.N., 2001. A higher-order sandwich plate theory accounting for 3-D stresses. International Journal of Solids and Structures 38, 5045–5062.

Palazotto, A.N., Linnemann, P.E., 1991. Vibration and buckling characteristics of composite cylindrical panels incorporating the effect of a higher order shear theory. International Journal of Solids and Structures 28, 341–361.

Seide, P., 1974. Reexamination of Koiter's theory of initial postbuckling behavior and imperfection sensitivity of structures. In: Thin Shell Structures: Theory, Experiment and Design. Prentice Hall, Englewood Cliffs, NJ, pp. 59–80.

Skvortsov, V., Bozhevolnaya, E., 2001. Two-dimensional analysis of shallow sandwich panels. Composite Structures 53, 43–53.

Sokolinsky, V., Frostig, Y., 2000. Branching behavior in the nonlinear response of sandwich panels with transversely flexible core. International Journal of Solids and Structures 37, 5745–5772.

Starlinger, A., Rammerstorfer, F.G., 1992. A finite element formulation for sandwich shells accounting for local failure phenomena. In: Sandwich Construction 2, Proceedings of the Second International Conference on Sandwich Construction. EMAS Publishing, Warley.

Vinson, J.R., 1999. The Behavior of Sandwich Structures of Isotropic and Composite Materials. Technomic Publishing, Lancaster, PA.

Vinson, J.R., 2001. Sandwich structures. Applied Mechanics Reviews 54, 201–214.

Wadee, M.A., Hunt, G.W., 1998. Interactively induced localized buckling in sandwich structures with core orthotropy. Journal of Applied Mechanics 65, 523–528.

Zenkert, D., 1997. An Introduction to Sandwich Construction. EMAS Publishing, Warley.